Charles University in Prague
Fakulty of Mathematics and Physics

DIPLOMA THESIS

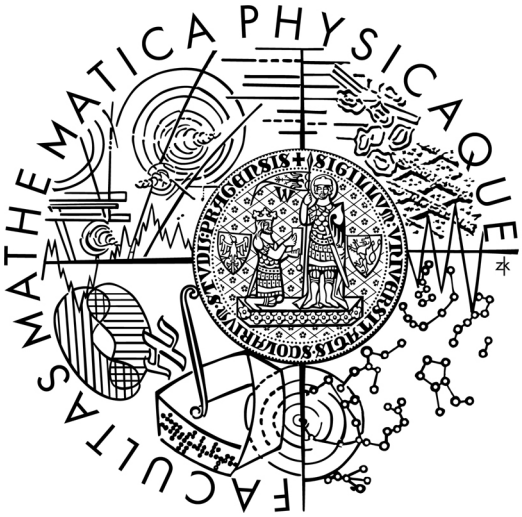

Petr Posolda

Study of exotic hypernuclei

Department of Theoretical Physics
Supervisor: RNDr. Jiří Mareš, CSc.
Study program: Theoretical physics

I am grateful to Jiří Mareš for supervising, useful comments, discussions and for careful reading of the manuscript.

I declare that I wrote the diploma thesis by myself and I used solely adduced references. I agree with lending of this work.

In Prague:

Contents:

ABSTRACT

Název práce: *Studium exotických hyperjader*
Autor: *Petr Posolda*
Katedra (ústav): *Ústav teoretické fyziky*
Vedoucí diplomové práce: *RNDr. Jiří Mareš, CSc., Ústav jaderný fyziky, AVČR, Řež*
e-mail vedoucího: *mares@ujf.cas.cz*

Abstrakt: *Diplomová práce se zabývá studiem vlastností exotických hyperjaderných systémů, konkrétně isotopů berylia, uhlíku, kyslíku a neonu za přítomnosti Λ a Σ hyperonu. Výpočty byly provedeny v rámci relativistické teorie středního pole (RMF), kde je (hyper)jádro popisována jako systém Diracových spinorů (nukleonů, hyperonů) interagujících prostřednictvím (středních) mezonových polí. Exotická hyperjádra byla popisována jako axiálně symetrická. Výpočty hyperjader byly dosud prováděny převážně za předpokladu sférické symetrie. Tato práce tedy rozšiřuje dosud známé předpovědi na oblast exotických, obecně deformovaných systémů. Pro uvedená hyperjádra byly provedeny numerické výpočty vazbových energií, středního kvadratického poloměru a studován vliv tenzorové interakce mezi ω mezonem a Λ hyperonem na spin orbitální rozštěpení Λ hyperonového energetického spektra. Potvrdilo se, že přítomnost Λ hyperonu zvyšuje hodnotu vazbové energie systému a naopak zmenšuje jeho střední kvadratický poloměr. Pro Σ hyperony byl výzkum zaměřen na možnost existence vázaných stavů Σ hyperonu v atomovém jádře. Ukázalo se, že pro zmíněné isotopy Σ^+ hyperjádro neexistuje, ale pro Σ^- hyperon vázané stavy v některých isotopech možné jsou.*

Klíčová slova: *Exotická hyperjádra, Λ(Σ) hyperon, RMF teorie, Diracova rovnice, Klein-Gordonova rovnice.*

Title: *Study of exotic hypernuclei*

Author: *Petr Posolda*

Department: *Department of Theoretical Physics*

Supervisor: *RNDr. Jiří Mareš, CSc.*, Nuclear Physics Institute, ASCR, Řež

Supervisor's e-mail address: *mares@ujf.cas.cz*

Abstract: *The thesis focuses on the study of properties of exotic hypernuclei, particularly of beryllium, carbon, oxygen and neon isotopes with Λ and Σ hyperons. Calculations were performed in the framework of the relativistic mean field theory (RMF) where a (hyper)nucleus is treated as a system of Dirac spinors (nucleons, hyperons) interacting via (mean) meson fields. The exotic hypernuclei were considered as axial symmetric. Up to now, hypernuclear calculations have been performed under assumption of spherical symmetry. This work thus extends hypernuclear calculations to the region of exotic, generally deformed systems. For the above nuclei, the numerical calculations of the binding energies and root mean square radii were performed. Moreover, we studied influence of the tensor interaction between ω meson and Λ hyperon on the Λ spin-orbit splitting. The results confirmed that the presence of the Λ hyperon increases values of the binding energy of a system and on the contrary, it decreases its root mean square radius. We studied the possibility of the existence of the Σ hyperon bound states in a nucleus. For the above isotopes, no bound states were found for the Σ^+ hyperons. On the other hand, weekly bound states of the Σ^- hyperon are predicted for several isotopes.*

Keywords: *Exotic hypernuclei, Λ(Σ) hyperon, RMF theory, Dirac equation, Klein-Gordon equation.*

1. Introduction

A hypernucleus is a nuclear system containing at least one hyperon, i.e. a baryon with nonzero strangeness. Since the hyperon is distinguishable from common nucleons, it represents in the nuclear medium an ideal and unique probe of the deep nuclear interior and makes possible to study mechanisms of various reactions by selecting particular channels marked by strangeness. The added hyperon gives a new dimension to the traditional nuclear world constituting a many-body baryon system (the hypernucleus becomes a first step to flavor nuclei). Hypernuclei also allow one to test directly nuclear models and models for baryon-baryon interaction in the strange sector. Week decays of hyperons give a tool for investigating week interactions and propagation of pions in the medium. Due to the special role of strangeness, hypernuclei may be well suited for investigation of (possible) subhadronic degrees of freedom. Strange particles (hyperons and possibly kaons) occur at a moderate density of about 2-3 times normal nuclear density in neutron stars matter [1]. These new particles influence the properties of the equation of state of the matter and consequently the global properties of neutron stars [2].

Exotic hypernuclei are hypernuclear isotopes with surplus or deficit of neutrons. The physics of nuclei in the vicinity of the neutron drip line has been studied in last decades and number of effects have been observed, e.g. a new type of clusters (neutron halo) and the N-Z dependence of NN interaction (shell occupancy). The Λ hyperon is known to make the nuclear core more stable, so Λ-hypernuclei have an interesting possibility of extending the neutron drip line from that obtained by ordinary nuclei [3, 4]. The experimental research of exotic Λ hypernuclei is nowadays under way in leading world laboratories. To mention a few, in KEK, the production of neutron-rich Λ-hypernucleus was observed [5]. The hypernuclei ${}^{10}_{\Lambda}\mathrm{Li}$ were detected as a product of the in-flight (π^-, K^+) double charge-exchange reaction on a ${}^{10}\mathrm{B}$ target. In Frascati (Italy), there was observed ${}^{6}_{\Lambda}\mathrm{H}$ and ${}^{7}_{\Lambda}\mathrm{H}$ in the (K^-_{stop}, π^+) reaction [6].

The vast majority of known experimental data is on Λ hypernuclei. Σ hypernuclei have been studied theoretically and have been searched for in CERN [7] and KEK [8, 9] experiments since eighties. Unfortunately, no Σ hypernuclear bound state has been confirmed in BNL experiments [10] with improved statistics, except ${}^{4}_{\Sigma}\mathrm{He}$. Moreover, the analysis of Σ atom data [11, 12] revealed that the central Σ-nucleus optical potential is repulsive inside the nucleus and only slightly attractive at the nuclear surface. On the other hand, the Σ hyperon, due to the Coulomb or isovector interaction, could be bound in an exotic nucleus.

Calculations of exotic Σ hypernuclei and investigations of their possible existence have not been performed yet.

In this thesis, the relativistic mean field (RMF) theory is used as a framework. The RMF theory as an approximation of quantum hadrodynamics (QHD) was proposed by Walecka in reference [13]. The model describes a nucleus as a system of Dirac nucleons interacting in a relativistic covariant manner via meson fields. The meson fields are treated as mean fields, i.e. as non-quantal c-number fields. Wide variety of nuclear applications has been successfully calculated within the RMF concept, which proved its applicability (for references see [14]). Since the first derivation of the RMF theory, several developments have been suggested to improve the original model. The introducing of the σ(ω)-meson nonlinear terms provided the correction of the nuclear compressibility and improved the description of the nuclear structure. The spin-orbit (s-o) interaction for the Λ hyperon is very small contrary to the s-o interaction for nucleons. The tensor interaction between the ω meson and the hyperon was included into the Lagrangian and the negligible Λ spin-orbit splitting was explained quite naturally using quark model [15, 16].

The RMF calculations of hypernuclei are mostly performed in assumption of spherical symmetry of the nuclear system. It is obvious that for exotic hypernuclei, i.e. strings of hypernuclear isotopes, it is desirable to consider deformation of these isotopes and therefore perform calculations assuming axial symmetry.

In the next section, we will present the RMF model, introduce the corresponding Lagrangian and derive equations of motion for the case of spherical and axial symmetry. In section 3, we will present parameterizations used in this work. The results of the calculations of Λ and Σ exotic hypernuclei are discussed in section 4. Finally, the conclusions are drawn in section 5.

2. Relativistic mean field theory for (hyper)nuclei

In the relativistic approach, the interaction between particles (baryons in our case) is not described by instantaneous force but it is mediated by fields, which are independent degrees of freedom. In the particular case, quantum hadrodynamics (QHD) [13], it is usual to consider meson fields with the lowest internal angular momentum J and isospin T. This presumption is in agreement with the spectrum of existing mesons and is justified also by the OBE potentials [17]. The fields taken into account are therefore scalar mesons (J=0) or vector mesons (J=1) and accordingly isoscalar (T=0) or isovector (T=1) mesons. Furthermore, as we are working with nuclear states having natural parity $\pi=(-1)^J$ the currents with unnatural parity will have zero expectation value in the RMF approximation [18]. Thus, π- and η-fields are not considered in this work. Consequently, the meson fields used in our approach are

- σ isoscalar - scalar field $\sigma(x^\mu)$
- ω isoscalar – vector field $\omega_\mu(x^\mu)$
- ρ isovector - vector field $\vec{\rho}^{\,\mu}(x^\mu)$
- γ massless vector field $A_\mu(x^\mu)$, the photon

The σ-field produces strong attraction between nucleons at medium range, the ω –field mediates short-range repulsion, the ρ-field adjusts the isovector properties of finite nuclei and the photon does the electromagnetic interaction.

Widely used approximation of QHD is the relativistic mean field theory (RMF) proposed by Walecka and Serot in ref. [13]. It is based on two main approximations. In order to illustrate these approximations, we present a very simple example with the Lagrangian density where nucleons ψ are coupled by just a scalar field

$$\mathcal{L} = \overline{\psi}\left(i\gamma^\mu\partial_\mu - M\right)\psi + \frac{1}{2}\left(\partial^\mu\sigma\,\partial_\mu\sigma - m_\sigma^2\sigma^2\right) - g_\sigma\overline{\psi}\psi\sigma\,, \tag{2.1}$$

In the *mean-field* approximation, the nucleons are treated as if they do not interact with each other directly, but they rather move mutually independently within the nuclei and their interaction is mediated by mean meson fields. Thus, even though this model is based on the

quantum field theory, the fields ψ and σ in (2.1) are not treated fully as quantum fields in the RMF model. The meson field operators are taken as their expectation value

$$\hat{\sigma} \to \langle \sigma \rangle =: \sigma \tag{2.2}$$

and therefore all meson fields are treated as classical c-number fields. Next, since the nucleons are moving mutually independently, the nucleon field operator $\hat{\psi}$ can be expanded in all times in terms of single particle states α as

$$\psi = \sum_{\alpha} \psi_{\alpha}(x^{\mu}) \hat{a}_{\alpha} \, . \tag{2.3}$$

Here $\hat{a}_{\alpha}$ is the annihilation operator for a nucleon in the state α and $\psi_{\alpha}(x^{\mu})$ is the single particle wave function. The corresponding scalar density can be written as

$$\langle : \overline{\psi}\psi : \rangle = \rho_{vac.pol.} + \sum_{\alpha=1}^{A} \overline{\psi}_{\alpha}\psi_{\alpha} \, , \tag{2.4}$$

where the first term isolates the vacuum polarization and the second one corresponds to the contribution of the A nucleons in a nucleus. To omit the first term means to neglect the quantum field effects and include only the summation over occupied particle states. This is the second, so-called *no-sea* approximation. Step by step derivation and reasoning of this approximation is given in refs. [13,18].

Finally, it is necessary to stress that all the introduced meson fields are only inspired by physical particles. Although their masses only slightly differ from them, in fact, they are phenomenological components of the RMF nuclear model. Their masses and coupling constants are fitted to the ground state properties of selected magic nuclei and nuclear matter characteristics. Several successful parameterizations have been developed so far and some of the most frequently used ones are applied in this work (see [19] for references).

2.1. Lagrangian density and equations of motion

Now, we will include into the Lagrangian density (2.1) the rest of the relevant meson fields and, of course, the hyperon part as well. This paper is concerned with Λ and Σ hyperons. Their main characteristics relevant for our calculations are listed in Table 1.

Table 1: Selected properties of hyperons considered in this work.

Particle	Mass [MeV]	Strangeness	Charge	Spin	Isospin
Λ	1115.6	-1	0	½	0
Σ^-	1189.4	-1	-1	½	1
Σ^0	1192.5	-1	0	½	1
Σ^+	1197.5	-1	1	½	1

Since all the above hyperons have spin ½, they will be described analogous to nucleons by a Dirac field. The Lagrangian density is a sum of the nucleon and hyperon part

$$\mathcal{L} = \mathcal{L}_N + \mathcal{L}_Y , \tag{2.1.1}$$

where Y=Σ Λ.

The nucleon part $\mathcal{L}_N$ is given by

$$\begin{aligned}
\mathcal{L}_N = & \bar{\psi}\left[i\gamma^\mu \partial_\mu - M \right]\psi \\
& + \frac{1}{2}\partial^\mu \sigma \partial_\mu \sigma - \frac{1}{2}m_\sigma^2 - U(\sigma) - g_{\sigma N}\bar{\psi}\ \psi\ \sigma \\
& - \frac{1}{4}\Omega^{\mu\nu}\Omega_{\mu\nu} + \frac{1}{2}m_\omega^2 \omega^\mu \omega_\mu - g_{\omega N}\bar{\psi}\ \gamma^\mu \psi \omega_\mu \\
& - \frac{1}{4}\vec{R}^{\mu\nu}\vec{R}_{\mu\nu} + \frac{1}{2}m_\rho^2 \vec{\rho}^\mu \vec{\rho}_\mu - g_{\rho N}\bar{\psi}\ \gamma^\mu \vec{\tau}\psi\ \vec{\rho}_\mu \\
& - \frac{1}{4}F^{\mu\nu}F_{\mu\nu} - e\bar{\psi}\ \gamma^\mu \frac{1-\tau_3}{2}\psi\ A_\mu ,
\end{aligned} \tag{2.1.2}$$

where the arrow denotes the isovector quantities. The potential U(σ) is a function

$$U(\sigma)=\frac{1}{3}g_2\sigma^3+\frac{1}{4}g_3\sigma^4 \tag{2.1.3}$$

including nonlinear self-coupling terms. This form was proposed by Boguta and Bodmer [20] to implement density dependence in order to improve the nuclear incompressibility, which comes out too large in the original Walecka model. The constants g_2 and g_3 are, of course, the others parameters of this model. The field tensors in (2.1.2) are given by

$$\begin{aligned}
&\Omega^{\mu\nu}=\partial^\mu\omega^\nu-\partial^\nu\omega^\nu \\
&\vec{R}^{\mu\nu}=\partial^\mu\vec{\rho}^\nu-\partial^\nu\vec{\rho}^\mu-g_\rho\left(\vec{\rho}^\mu\times\vec{\rho}^\nu\right) \\
&F^{\mu\nu}=\partial^\mu A^\nu-\partial^\nu A^\mu .
\end{aligned} \tag{2.1.4}$$

Here, M, m_σ, m_ω, m_ρ are the masses of the nucleon, σ-meson, ω-meson and ρ-meson respectively, and $g_{\sigma N}$, $g_{\omega N}$, $g_{\rho N}$ are the corresponding coupling constants.

The hyperon part $\mathcal{L}_Y$ is

$$\mathcal{L}_Y=\overline{\psi}_Y\left[i\gamma_\mu\partial^\mu-g_{\omega Y}\gamma_\mu\omega^\mu-\left(M_Y+g_{\sigma Y}\sigma\right)\right]\psi_Y+\mathcal{L}_T+\mathcal{L}_{\rho Y}+\mathcal{L}_{AY}, \tag{2.1.5}$$

where M_Y is the mass of a hyperon, $g_{\sigma Y}$ ($g_{\omega Y}$) is the coupling constant for σ-, ω- meson-hyperon interaction.

The term

$$L_T=\frac{f_{\omega Y}}{2M_Y}\overline{\psi}_Y\sigma^{\mu\nu}\left(\partial_\nu\omega_\mu\right)\psi_Y \tag{2.1.6}$$

represents the tensor interaction between the ω meson and a hyperon and $\sigma^{\mu\nu}=\frac{i}{2}\left[\gamma^\mu,\gamma^\nu\right]$.

The last two terms describe the hyperon interaction with the ρ-meson and photon. Since Λ is a neutral, I=0 particle

$$\mathcal{L}_{\rho\Lambda}=\mathcal{L}_{A\Lambda}=0 . \tag{2.1.7}$$

In the case of a Σ-hyperon

$$\mathcal{L}_{\rho\Sigma}+\mathcal{L}_{A\Sigma}=-\overline{\Sigma}_{ij}\left(\frac{g_{\rho\Sigma}}{2}\gamma_\mu\Theta^\mu_{jk}+\frac{e}{2}\gamma_\mu A^\mu\left(\tau_3,\Sigma\right)_{jk}\right)\Sigma_{ki}, \tag{2.1.8}$$

where

$$\Sigma=\begin{pmatrix}\psi_{\Sigma^0} & \sqrt{2}\psi_{\Sigma^+}\\ \sqrt{2}\psi_{\Sigma^-} & -\psi_{\Sigma^0}\end{pmatrix} \text{ and } \Theta^\mu=\begin{pmatrix}\rho_0^\mu & \sqrt{2}\rho_+^\mu\\ \sqrt{2}\rho_-^\mu & -\rho_0^\mu\end{pmatrix} \quad [21]. \tag{2.1.9}$$

Before deriving equations of motion for the above Lagrangian, we make use of further simplifying assumptions, which make calculations considerably easier. Since we are interested in stationary states all time derivatives of densities and fields vanish

$$\dot{\sigma}=0,\ \dot{\omega}_\mu=0,\ \dot{\vec{\rho}}_\mu=0,\dot{A}_\mu=0 \tag{2.1.10}$$

and all the spatial components of 4-vectors are zero as well

$$\omega_i=0,\ \vec{\rho}_i=0,\ A_i=0\text{, where i=1,2,3} \quad [18]. \tag{2.1.11}$$

Further, we assume that the single particle states are pure proton or pure neutron states so they do not mix isospin. Consequently, we take into account only the third, neutral component of the isovector meson ρ. The remaining meson fields are therefore σ, ω_0, A_0 and $\rho^0{}_0$, which we will denote simply ρ^0 and they are all time independent. Finally, the single particle wave function has a form

$$\psi_i(r,t)\approx\exp\left(\mathrm{i}\varepsilon_i t\right)\psi_i(\vec{r}), \tag{2.1.12}$$

where ε_i is the single particle energy.

The next step is to derive the equations of motion from the Lagrangian density (2.1.1) by using Hamilton variational principle. With all the above simplifications, we obtain:

$$\left[-i\vec{\alpha}\cdot\vec{\nabla}+\beta\left(M+g_{\sigma N}\sigma\right)+g_{\omega N}\omega^0+g_{\rho N}\tau_3\rho^0+e\frac{1-\tau_3}{2}A^0\right]\psi_i=\varepsilon_i\psi_i \tag{2.1.13}$$

$$\begin{aligned}&\left[-i\vec{\alpha}\cdot\vec{\nabla}+g_{\omega Y}\omega^0+\beta\left(M_Y+g_{\sigma Y}\sigma\right)+\frac{f_{\omega Y}}{2M_Y}\beta\vec{\alpha}\cdot\left(i\vec{\nabla}\omega^0\right)\right]\psi_Y\\&+\delta_{Y\Sigma^+}\left(g_{\rho\Sigma}\psi_Y\rho^0+e\psi_YA^0\right)-\delta_{Y\Sigma^-}\left(g_{\rho\Sigma}\psi_Y\rho^0+e\psi_YA^0\right)=\varepsilon_Y\psi_Y\end{aligned} \tag{2.1.14}$$

$$\left(-\Delta+m_\sigma^2\right)\sigma=-g_2\sigma^2-g_3\sigma^3-\sum_i g_{\sigma N}\overline{\psi}_i\psi_i-g_{\sigma Y}\overline{\psi}_Y\psi_Y \tag{2.1.15}$$

$$\left(-\Delta+m_\omega^2\right)\omega^0=\sum_i g_{\omega N}\overline{\psi}_i\beta\psi_i+g_{\omega Y}\overline{\psi}_Y\beta\psi_Y+i\frac{f_{\omega Y}}{2M_Y}\vec{\nabla}\left(\overline{\psi}_Y\vec{\alpha}\psi_Y\right) \tag{2.1.16}$$

$$\left(-\Delta+m_\rho^2\right)\rho^0=\sum_i g_{\omega N}\overline{\psi}_i\gamma^0\tau_3\psi_i+g_{\sigma\Sigma}\overline{\psi}_{\Sigma^+}\gamma^0\psi_{\Sigma^+}-g_{\sigma\Sigma}\overline{\psi}_{\Sigma^-}\gamma^0\psi_{\Sigma^-} \tag{2.1.17}$$

$$-\Delta A^0=\sum_i e\overline{\psi}_i\beta\frac{1-\tau_3}{2}\psi_i+e\overline{\psi}_{\Sigma^+}\gamma^0\psi_{\Sigma^+}-e\overline{\psi}_{\Sigma^-}\gamma^0\psi_{\Sigma^-}. \tag{2.1.18}$$

Let us denote the nucleon densities as

$$\begin{aligned}\rho_{\sigma N}(\vec{r})&=\sum_{i=1}^{A}\overline{\psi}_i(\vec{r})\psi_i(\vec{r})\\\rho_{\omega N}(\vec{r})&=\sum_{i=1}^{A}\psi_i^+(\vec{r})\psi_i(\vec{r})\\\rho_{3N}(\vec{r})&=\sum_{i=1}^{A}\psi_i^+(\vec{r})\tau_3\psi_i(\vec{r})\\\rho_{pN}(\vec{r})&=\sum_{i=1}^{A}\psi_i^+(\vec{r})\frac{1-\tau_3}{2}\psi_i(\vec{r})\\j_{AN}(\vec{r})&=\sum_{i=1}^{A}\overline{\psi}_i\,\beta(\vec{r})\frac{1-\tau_3}{2}\psi_i(\vec{r}),\end{aligned} \tag{2.1.19}$$

and the hyperon densities as

$$\begin{aligned}
&\rho_{\sigma Y}(\vec{r}) = \overline{\psi}_Y(\vec{r})\psi_Y(\vec{r}) \\
&\rho_{\omega Y}(\vec{r}) = \psi_Y^+(\vec{r})\psi_Y(\vec{r}) \\
&\rho_{\omega-Y}^T(\vec{r}) = \vec{\nabla}\left(\overline{\psi}_Y\vec{\alpha}\psi_Y\right) \\
&\rho_{3Y}(\vec{r}) = \psi_Y^+(\vec{r})\tau_3\psi_Y(\vec{r}) \\
&\rho_{pY}(\vec{r}) = \psi_Y^+(\vec{r})\frac{1-\tau_3}{2}\psi_Y(\vec{r}) \\
&j_{AY}(\vec{r}) = \overline{\psi}_{\Sigma^+}\gamma^0\psi_{\Sigma^+} - e\,\overline{\psi}_{\Sigma^-}\gamma^0\psi_{\Sigma^-}.
\end{aligned} \tag{2.1.20}$$

The first and the second equation (2.1.8) is the Dirac equation for nucleons and hyperon, respectively. Next three equations (2.1.9) to (2.1.11) are inhomogeneous Klein-Gordon equations for individual meson fields with sources given by corresponding baryon densities on the right-hand side. Equation (2.1.12) is for the photons where the sources are given by densities of all considered fields for charged particles. From the above system of coupled equations of motion, it can be clearly seen the essence of the RMF theory of nuclear interaction. Namely, the baryons interact only via the mean meson fields. As sources in the Klein-Gordon equations, the baryons generate meson fields and the meson fields on the contrary influence the relevant baryon densities via potential terms in the Dirac equations.

The solution of the set of equations (2.1.13 – 2.1.18) has to be carried out iteratively. Starting from the reasonable estimate of the meson fields, we can solve the Dirac equations (2.1.13) and (2.1.14). We obtain the spinors, i.e. the orbits in which the baryons move in presence of the meson fields. If we consider that A nucleons occupy the lowest particle levels, we obtain from equations (2.1.19) the densities by summation over these levels. The hyperon densities are obtained immediately from eq. (3.2.20). The solution of the Klein-Gordon equations (2.1.15) – (2.1.18) using these sources gives us new meson fields and new electromagnetic field, which can be used to calculate the potentials and effective mass in the Dirac equations. The solution of the Dirac equations with these new fields gives us Dirac spinors for the next iteration.

From the solution, we can calculate the total energy, which, in the static case, has the form:

$$E = \int d^3r\, \mathcal{H}(\vec{r}), \tag{2.1.21}$$

where

$$\mathcal{H}(\vec{r}) = \sum_i \psi_i^+ \left[-i\vec{\alpha}\cdot\vec{\nabla} + \beta\left(M + g_{\sigma N}\sigma\right) + g_{\omega N}\omega^0 + g_\rho \tau_3 \rho^0 + e\frac{1-\tau_3}{2}A^0 \right]\psi_i +$$
$$+\overline{\psi}_Y \left[-i\vec{\alpha}\cdot\vec{\nabla} + g_{\omega Y}\omega^0 + \beta\left(M_Y + g_{\sigma Y}\sigma\right) - \frac{f_{\omega Y}}{2M_Y}\vec{\alpha}\cdot\left(i\vec{\nabla}\omega^0\right) \right]\psi_Y$$
$$+\delta_{Y\Sigma^+}\psi_Y^+\psi_Y\left(g_{\rho\Sigma}\rho^0 + eA^0\right) - \delta_{Y\Sigma^-}\psi_Y^+\psi_Y\left(g_{\rho\Sigma}\rho^0 - eA^0\right) +$$
$$+\frac{1}{2}(\nabla\sigma)^2 + \frac{1}{2}m_\sigma^2\sigma^2 + U(\sigma) -$$
$$-\frac{1}{2}\left(\nabla\omega^0\right)^2 + \frac{1}{2}m_\omega^2\left(\omega^0\right)^2$$
$$-\frac{1}{2}\left(\nabla\rho^0\right)^2 + \frac{1}{2}m_\rho^2\left(\rho^0\right)^2 -$$
$$-\frac{1}{2}\left(\nabla A^0\right)^2$$

2.2 Spherical symmetry

If we assume the spherical symmetry for nuclei, the common coordinates are

$$\begin{aligned} x &= r\sin\upsilon\cos\phi \qquad & r &\in (0,\infty) \\ y &= r\sin\upsilon\sin\phi \qquad & \upsilon &\in (0,\pi) \\ z &= r\cos\upsilon \qquad & \phi &\in (0,2\pi). \end{aligned} \tag{2.2.1}$$

In this case, all densities on the right-hand side of Klein-Gordon equations as well as the meson fields are considered dependent only on the radial coordinate r.

The equations (2.1.13) and (2.1.18) define the single particle Dirac Hamiltonian that can be written as

$$h = -i\vec{\alpha}\cdot\vec{\nabla} + \beta M^*(r) + V(r), \tag{2.2.2}$$

where

$$M^*(\vec{r}) = M_i + g_{\sigma i}\sigma$$
$$V(\vec{r}) = g_{\omega i}\omega^0 + I_{3i}g_{\rho i}\rho^0 + Q_i eA^0 \tag{2.2.3}$$

for

$$\begin{aligned} I_{3i} &= \tau_3 \quad for\ i = N \\ &\quad 1,0,-1 \quad for\ i = \Sigma^+, \Sigma^0(\Lambda), \Sigma^- \\ Q_i &= \frac{1}{2}(1-\tau_3) \quad for\ i = N \\ &\quad I_3 \quad for\ \ i = \Sigma(\Lambda). \end{aligned} \tag{2.2.4}$$

Dirac equations then acquire general form

$$\left[-i\vec{\alpha}\cdot\vec{\nabla} + \beta M^*(r) + V(r)\right]\psi(r,\theta,\varphi) = \varepsilon\psi(r,\theta,\varphi). \tag{2.2.5}$$

The standard way of solution of a Dirac equation with the spherically symmetric potential is based on the separation of the angular and radial part. The commutation relations for operators $\vec{J}, \vec{L}, \vec{S}$ determine the angular part of the wave function. (Operators $\vec{J}, \vec{L}, \vec{S}$ are well known operators of the total angular momentum, angular momentum and spin respectively). Since the process of the solution of the angular part can be found in many publications (for example [13,22]), we will adopt the result from ref. [13] and will go through the radial part only.

The solution of the angular part is given by spin spherical harmonics

$$\varphi_{\kappa m} = \sum_{m_l, m_s} \left\langle\ l m_l \frac{1}{2} m_s \right|\ l \frac{1}{2}\ jm\ \left\rangle Y_{lm_l}(\zeta,\phi)\chi_{m_s}\right. \tag{2.2.6}$$

$$j = |\kappa| - \frac{1}{2}, \qquad l = \begin{cases} \kappa, & \kappa > 0 \\ -(\kappa+1), & \kappa < 0 \end{cases}$$

where Y_{lm_l} is a spherical harmonics and χ_{m_s} is a two-component Pauli spinor and $\left\langle\ l m_l \frac{1}{2} m_s \right|\ l \frac{1}{2}\ jm\ \left\rangle\right.$ are Clebsch-Gordon coefficients. The quantum number κ is the eigenvalue of operator K,

$$K = \beta\left(2\vec{\Sigma}\cdot\vec{J} - 1/2\right). \tag{2.2.7}$$

The equations

$$\begin{aligned} l_A(l_A+1) &= \kappa + j(j+1) + 1/4 \\ l_B(l_B+1) &= -\kappa + j(j+1) + 1/4 \end{aligned} \tag{2.2.8}$$

relate κ with eigenvalues of the angular momentum l_A (l_B) for the upper (lower) components of the Dirac bispinor. For given κ and j, the numbers l_A and l_B differ by one and l_A and l_B must be $j \pm ½$.

The single particle wave function is therefore written as

$$\psi_{n\kappa m}(\vec{x}) = \begin{pmatrix} R_{1n\kappa}(r)\varphi_{\kappa m}(\vec{n}) \\ R_{2n\kappa}(r)\varphi_{-\kappa m}(\vec{n}) \end{pmatrix}, \tag{2.2.9}$$

where n denotes the principal quantum number and $\vec{n} = \dfrac{\vec{x}}{|\vec{x}|}$.

Now we focus on the radial part. The expression (2.2.9) can be rewritten into [22]

$$\psi_{n\kappa m}(\vec{x}) = \begin{pmatrix} R_{1n\kappa}(r)\varphi_{\kappa m}(\vec{n}) \\ R_{2n\kappa}(r)(\vec{n}\cdot\vec{\sigma})\varphi_{\kappa m}(\vec{n}) \end{pmatrix}. \tag{2.2.10}$$

Then for a Dirac equation of the form $(h-\varepsilon)\psi = 0$ we obtain

$$\begin{pmatrix} M^* + V - \varepsilon & \vec{\sigma}\cdot\vec{p} \\ \vec{\sigma}\cdot\vec{p} & -M^* + V - \varepsilon \end{pmatrix} \begin{pmatrix} R_{1n\kappa}\varphi_{\kappa m} \\ R_{2n\kappa}(\vec{\sigma}\cdot\vec{n})\varphi_{\kappa m} \end{pmatrix} = 0, \tag{2.2.11}$$

where $\vec{p}$ is the momentum operator. A straightforward calculation leads to

$$\begin{aligned} \left[(M^* + V - E)R_{1n\kappa} + (\vec{\sigma}\cdot\vec{p})(\vec{\sigma}\cdot\vec{n})R_{2n\kappa}\right]\varphi_{\kappa m} &= 0 \\ \left[(\vec{\sigma}\cdot\vec{p})R_{1n\kappa} + (-M^* + V - E)(\vec{\sigma}\cdot\vec{n})R_{2n\kappa}\right]\varphi_{\kappa m} &= 0 \end{aligned} \tag{2.2.12}$$

Multiplying the second equation from the left side by $(\vec{\sigma}\cdot\vec{n})$ and using general relations

$$(\vec{\sigma}\cdot\vec{p})(\vec{\sigma}\cdot\vec{n})f=-i\frac{1}{r}(2+r\frac{\partial}{\partial r}+\vec{\sigma}\cdot\vec{L})f$$
$$(\vec{\sigma}\cdot\vec{n})(\vec{\sigma}\cdot\vec{p})f=-i\frac{1}{r}(r\frac{\partial}{\partial r}-\vec{\sigma}\cdot\vec{L})f \qquad (2.2.13)$$

which can be easily proved with using the relation $(\vec{\sigma}\cdot\vec{a})(\vec{\sigma}\cdot\vec{b})=\vec{a}\cdot\vec{b}+i\vec{\sigma}(\vec{a}\times\vec{b})$, we obtain

$$\left[(M^{*}+V-E)R_{1n\kappa}-i\frac{1}{r}(2+r\frac{\partial}{\partial r}+\vec{\sigma}\cdot\vec{L})R_{2n\kappa}\right]\varphi_{\kappa m}=0$$
$$\left[(-M^{*}+V-E)R_{n\kappa 2}-i\frac{1}{r}(r\frac{\partial}{\partial r}-\vec{\sigma}\cdot\vec{L})R_{1n\kappa}\right]\varphi_{\kappa m}=0 \qquad (2.2.14)$$

The term $\vec{\sigma}\cdot\vec{L}$ affects only the $\varphi_{\kappa m}$, so

$$(\vec{\sigma}\cdot\vec{L})\varphi_{\kappa m}=(\mathbf{J}^{2}-\mathbf{L}^{2}-\mathbf{S}^{2})\varphi_{\kappa m}=-(1+\kappa)\varphi_{\kappa m}. \qquad (2.2.15)$$

Inserting this result into the (2.2.14) we get

$$(M^{*}+V-E)R_{1n\kappa}-i\frac{1}{r}(1-\kappa^{\pm}+r\frac{\partial}{\partial r})R_{2n\kappa}=0$$
$$(-M^{*}+V-E)R_{2n\kappa}-i\frac{1}{r}(1+\kappa^{\pm}+r\frac{\partial}{\partial r})R_{1n\kappa v}=0 \qquad (2.2.16)$$

Comparing equations (2.2.16) with the analogous equations (3.7) in ref. [23], one can notice that they differ by the sign in front of the term $i(1-\kappa^{\pm}+r\frac{\partial}{\partial r})R_{2n\kappa}$. We are convinced that there is an error in ref. [23].

The equations (2.2.16) have to be solved for all the occupied nucleon levels in the nucleus. The solutions ψ_i (i=1,..,A) determine the densities (2.1.19)

$$\begin{aligned}
\rho_\sigma(r) &= \sum_i \left(|R_{1i}(r)|^2 - |R_{2i}(r)|^2 \right) \\
\rho_\omega(r) &= \sum_i \left(|R_{1i}(r)|^2 + |R_{2i}(r)|^2 \right) \\
\rho_3(r) &= \sum_i \left(|R_{1i}(r)|^2 + |R_{2i}(r)|^2 \right) \\
\rho_p(r) &= \sum_i \left(|R_{1i}(r)|^2 + |R_{2i}(r)|^2 \right)
\end{aligned} \tag{2.2.17}$$

The densities (2.2.17) are the sources in the Klein-Gordon equations (2.1.15) to (2.1.18) for the corresponding fields σ(r), ω^0(r), ρ^0(r) and A^0(r). The Klein-Gordon equation in spherical coordinates (2.2.1) is

$$\left(-\frac{\partial^2}{\partial r^2} - \frac{2}{r}\frac{\partial}{\partial r} + m_\phi^2 \right) \phi(r) = s_{\phi N}(r) + s_{\phi Y}(r) . \tag{2.2.18}$$

Here, m_ϕ are the meson masses for $\phi = \sigma, \omega, \rho$ and zero for the photon. The sources then correspond to

$$s_{\phi N}(r) = \begin{cases} -g_\sigma \rho_s(r) - g_2 \sigma^2(r) - g_3 \sigma^3(r) & \text{for the } \sigma-\text{field} \\ g_\omega \rho_\omega(r) & \text{for the } \omega-\text{field} \\ g_\rho \rho_3(r) & \text{for the } \rho-\text{field} \\ e\rho_p(r) & \text{for the } A-\text{field} \end{cases} \tag{2.2.19}$$

The hyperon source part is similar. Since we consider only one hyperon in its ground state 1s½, the sources for respective fields are obviously very simple

$$s_{\phi Y}(r) = \begin{cases} \rho_{\sigma Y}(r) = \left(|R_{1i}(r)|^2 - |R_{2i}(r)|^2 \right) \\ \rho_{\omega Y}(r) = \left(|R_{1i}(r)|^2 + |R_{2i}(r)|^2 \right) \\ \rho_{3Y}(r) = \left(|R_{1i}(r)|^2 + |R_{2i}(r)|^2 \right) \\ \rho_{pY}(r) = \left(|R_{1i}(r)|^2 + |R_{2i}(r)|^2 \right) \end{cases} \tag{2.2.20}$$

The equations (2.2.16) and (2.2.18) are coupled nonlinear differential equations that may be solved by an iterative procedure. For a given set of meson fields, the Dirac equation (2.2.16) is solved iteratively by Runge-Kutta method outward from the origin and inward

from large r, matching the solution at an intermediate radius to determine the eigenvalues ε_i. Analytic solutions in the region of large and small r allow the proper boundary conditions to be imposed.

Once the baryon wave functions are determined, the source terms (2.2.19) and (2.2.20) may be calculated and the meson fields recomputed by integrating over the corresponding static Green's function. Inserting the determined meson fields into the Dirac equations, we solve the Dirac equations and obtain new set of wave functions. We compute the new densities and repeat the whole procedure until the self-consistency is achieved.

2.3. Axial symmetry

The assumption of spherical symmetry is not appropriate for every nucleus. Nuclei with open energy shells are often (sometimes appreciably) deformed. Such nuclei are usually described by axially symmetric shapes [23], using cylindrical coordinates

$$\begin{aligned} x &= r_\perp \cos\varphi \\ y &= r_\perp \sin\varphi \\ z &= z. \end{aligned} \tag{2.3.1}$$

Let us consider that the densities are invariant with respect to rotation around the z axis. The spinor ψ is in this case characterized by the quantum numbers $\Omega = m_l + m_s$ the eigenvalue of the symmetry operator J_z, parity π and isospin t.

In the following subsection, we will derive Dirac equations and Klein-Gordon equations for the axially symmetric case. This time we will solve the equations of motion by expansion in the basis of an axially symmetric harmonic oscillator. The problem then reduces to finding the coefficients of this expansion.

2.3.1 Numerical solution of Dirac equation

For simplicity, we will first consider the case without the tensor interaction. The Dirac equation can be again written as

$$\left[-i\begin{pmatrix}0 & \vec{\sigma}\\ \vec{\sigma} & 0\end{pmatrix}\vec{\nabla}+\begin{pmatrix}1 & 0\\ 0 & -1\end{pmatrix}M^{*}+\begin{pmatrix}1 & 0\\ 0 & 1\end{pmatrix}V\right]\psi=\varepsilon\psi \tag{2.3.1.1}$$

where the mass M^* and the potential V has the same form (2.2.3) and (2.2.4) as in the spherical case with the exception that the meson fields now depend on the coordinates $r_\perp, z$. After inserting the ansatz [23]

$$\psi(\vec{r},t)=\frac{1}{\sqrt{2\pi}}\begin{pmatrix} f^{+}(z,r_\perp)e^{i\left(\Omega-\frac{1}{2}\right)\varphi}\\ f^{-}(z,r_\perp)e^{i\left(\Omega+\frac{1}{2}\right)\varphi}\\ ig^{+}(z,r_\perp)e^{i\left(\Omega-\frac{1}{2}\right)\varphi}\\ ig^{-}(z,r_\perp)e^{i\left(\Omega+\frac{1}{2}\right)\varphi}\end{pmatrix}\chi_t(t) \tag{2.3.1.2}$$

into (2.3.1.1), straightforward calculation leads to

$$\begin{aligned}
&\left(M^{*}+V\right)f^{+}+\partial_z g^{+}+\left(\partial_{r_\perp}+\frac{\Omega+1/2}{r_\perp}\right)g^{-}=\varepsilon f^{+}\\
&\left(M^{*}+V\right)f^{-}-\partial_z g^{-}+\left(\partial_{r_\perp}-\frac{\Omega-1/2}{r_\perp}\right)g^{+}=\varepsilon f^{-}\\
&\left(M^{*}-V\right)g^{+}+\partial_z f^{+}+\left(\partial_{r_\perp}+\frac{\Omega+1/2}{r_\perp}\right)f^{-}=-\varepsilon g^{+}\\
&\left(M^{*}-V\right)g^{-}-\partial_z f^{-}+\left(\partial_{r_\perp}-\frac{\Omega-1/2}{r_\perp}\right)f^{+}=-\varepsilon g^{-}\,.
\end{aligned} \tag{2.3.1.3}$$

Next, we expand the spinors $f^{\pm}$ and $g^{\pm}$ in terms of the eigenfunctions of a deformed axially symmetric oscillator. They can be written explicitly as [23]

$$\Phi_\alpha(z,r_\perp,\varphi,s,t)=\phi_{n_z}(z)\phi_{n_r}^{m_l}(r)\frac{1}{\sqrt{2\pi}}e^{im_l\varphi}\chi_{m_s}(s), \tag{2.3.1.4}$$

where

$$\begin{aligned}\phi_{n_z}(z)&=\frac{N_{n_z}}{\sqrt{b_z}}H_{n_z}(\xi)e^{-\xi^2/2}\\ \phi_{n_r}^{m_l}(r_\perp)&=\frac{N_{n_r}^{m_l}}{b_\perp}\sqrt{2}\eta^{|m_l|/2}L_{n_r}^{|m_l|}(\eta)e^{-\eta/2}\end{aligned} \tag{2.3.1.5}$$

and where the $H_{n_z}(\xi)$ are Hermite polynomials and $L_{n_r}^{|m_l|}(\eta)$ are the associated Laguerre polynomials as defined in [24]. The new variables ζ and η obey

$$\xi=\frac{z}{b_z},\qquad \eta=\frac{r_\perp^2}{b_\perp^2} \tag{2.3.1.6}$$

and the normalization constants are given by

$$N_{n_z}=\frac{1}{\sqrt{\sqrt{\pi}2^{n_z}n_z!}},\qquad N_{n_r}^{m_l}=\sqrt{\frac{n_{r_\perp}!}{(n_{r_\perp}+m_l)!}}. \tag{2.3.1.7}$$

The choice of the oscillator length parameters b_z, $b_\perp$ and their role in numerical solutions is discussed in ref. [23]. The expansion (2.3.1.2) into eigenstates of the harmonic oscillator is explicitly written as

$$\psi(\vec{r},t)=\frac{1}{\sqrt{2\pi}}\begin{pmatrix}f^+(z,r_\perp)e^{i\left(\Omega-\frac{1}{2}\right)\varphi}\\ f^-(z,r_\perp)e^{i\left(\Omega+\frac{1}{2}\right)\varphi}\\ ig^+(z,r_\perp)e^{i\left(\Omega-\frac{1}{2}\right)\varphi}\\ ig^-(z,r_\perp)e^{i\left(\Omega+\frac{1}{2}\right)\varphi}\end{pmatrix}\chi_t(t)=\begin{pmatrix}\sum_{\alpha}^{\alpha_{max}}f_\alpha\Phi_\alpha(\vec{r},s)\chi_t(t)\\ \sum_{\tilde{\alpha}}^{\tilde{\alpha}_{max}}f_{\tilde{\alpha}}\Phi_{\tilde{\alpha}}(\vec{r},s)\chi_t(t)\end{pmatrix}. \tag{2.3.1.8}$$

We insert it into equation (2.3.1.3) and we obtain

$$\begin{bmatrix} M^*+V & 0 & \partial_z & \partial_{r_\perp}+\dfrac{\Omega+1/2}{r_\perp} \\ 0 & M^*+V & \partial_{r_\perp}-\dfrac{\Omega-1/2}{r_\perp} & -\partial_z \\ \partial & \partial_{r_\perp}+\dfrac{\Omega+1/2}{r_\perp} & M^*-V & 0 \\ \partial_{r_\perp}-\dfrac{\Omega-1/2}{r_\perp} & -\partial_z & 0 & M^*-V \end{bmatrix} \begin{bmatrix} \sum_{\alpha}^{\alpha_{\max}} f_\alpha \Phi_\alpha(\vec{r},s)\chi_t(t) \\ \sum_{\alpha}^{\alpha_{\max}} f_\alpha \Phi_\alpha(\vec{r},s)\chi_t(t) \\ \sum_{\tilde{\alpha}}^{\tilde{\alpha}_{\max}} f_{\tilde{\alpha}} \Phi_{\tilde{\alpha}}(\vec{r},s)\chi_t(t) \\ \sum_{\tilde{\alpha}}^{\tilde{\alpha}_{\max}} f_{\tilde{\alpha}} \Phi_{\tilde{\alpha}}(\vec{r},s)\chi_t(t) \end{bmatrix} = \varepsilon \begin{bmatrix} \sum_{\alpha}^{\alpha_{\max}} f_\alpha \Phi_\alpha(\vec{r},s)\chi_t(t) \\ \sum_{\alpha}^{\alpha_{\max}} f_\alpha \Phi_\alpha(\vec{r},s)\chi_t(t) \\ \sum_{\tilde{\alpha}}^{\tilde{\alpha}_{\max}} f_{\tilde{\alpha}} \Phi_{\tilde{\alpha}}(\vec{r},s)\chi_t(t) \\ \sum_{\tilde{\alpha}}^{\tilde{\alpha}_{\max}} f_{\tilde{\alpha}} \Phi_{\tilde{\alpha}}(\vec{r},s)\chi_t(t) \end{bmatrix} \tag{2.3.1.9}$$

Now we use the ortogonality relations of the eigenstates of the harmonic oscillator (see appendix A). We multiply each row in (2.3.1.9) by eigenstate $\langle \Phi_{\alpha'} |$ and we obtain the following equation for the coefficients f_α and $g_{\tilde{\alpha}}$

$$\begin{pmatrix} A_{\alpha,\alpha'} & B_{\tilde{\alpha},\alpha'} \\ B_{\alpha,\tilde{\alpha}'} & -C_{\tilde{\alpha},\tilde{\alpha}'} \end{pmatrix} \begin{pmatrix} f_\alpha \\ g_{\tilde{\alpha}} \end{pmatrix} = \varepsilon \begin{pmatrix} f_\alpha \\ -g_{\tilde{\alpha}} \end{pmatrix}. \tag{2.3.1.10}$$

If we determine the matrix elements $A_{\alpha,\alpha'}, B_{\alpha,\alpha'}$ and $C_{\alpha,\alpha'}$ the whole problem reduces to the solution of the algebraical equation (2.3.1.10) for unknown f_α and $g_{\tilde{\alpha}}$. For the matrix elements $A_{\alpha,\alpha'}, C_{\alpha,\alpha'}$ we get

$$\begin{aligned} \begin{pmatrix} A_{\alpha,\alpha'} \\ C_{\alpha,\alpha'} \end{pmatrix} &= \delta_{m_s,m_s'}\delta_{m_l,m_l'} N_{n_z} N_{n_z'} N_{n_r}^{|m_l|} N_{n_r'}^{|m_l'|} \int_{-\infty}^{\infty} d\zeta e^{-\zeta^2} H_{n_z}(\zeta) H_{n_z'}(\zeta) \\ &\times \int_0^{\infty} d\eta \eta^{|m_l|} e^{-\eta} L_{n_r}^{|m_l|}(\eta) L_{n_r'}^{|m_l'|}(\eta) \left[M^*\left(b_z\zeta, b_\perp\sqrt{\eta}\right) \pm V\left(b_z\zeta, b_\perp\sqrt{\eta}\right) \right] \end{aligned} \tag{2.3.1.11}$$

The computation of $B_{\alpha,\alpha'}$ is more complicated due to terms with derivatives. Main steps of the evaluation are shown in appendix A. The resulting expression for $B_{\alpha,\alpha'}$ is:

$$B_{\alpha,\alpha'} = \delta_{n_r,n'_r}\delta_{m_l,m'_l}\delta_{m_s,m'_s}\frac{(-1)^{\frac{1}{2}+m_s}}{b_z}\left[\sqrt{\frac{n'_z}{2}}\delta_{n'_z,n_z+1} - \sqrt{\frac{n_z}{2}}\delta_{n'_z,n_z-1}\right] +$$
$$+\delta_{n_z,n'_z}\frac{N_{n_r}^{|m_l|}N_{n'_r}^{|m'_l|}}{2}\delta_{m_s,m'_s+1}\delta_{m_l,m'_l-1}\int_0^\infty d\eta\, e^{-\eta}\eta^{m_l}\left[\tilde{L}_{n_r}^{|m_l|}(\eta) - m_l L_{n_r}^{|m_l|}(\eta)\right]L_{n'_r}^{|m'_l|}(\eta) \qquad (2.3.1.12)$$
$$+\delta_{n_z,n'_z}\frac{N_{n_r}^{|m_l|}N_{n'_r}^{|m'_l|}}{2}\delta_{m_s,m'_s-1}\delta_{m_l,m'_l+1}\int_0^\infty d\eta\, e^{-\eta}\eta^{m_l-1}\left[\tilde{L}_{n_r}^{|m_l|}(\eta) + m_l L_{n_r}^{|m_l|}(\eta)\right]L_{n'_r}^{|m'_l|}(\eta).$$

Here is to be noted that we found errors in the expression for $B_{\alpha,\alpha'}$ (eq. 4.27) in ref. [23]. Now we add the tensor interaction to the equation of motion. We neglect the tensor term for nucleons as the coupling constant $f_{\omega N}$ is ≈ 0 and we consider only the tensor term for a hyperon. Its contribution leads to the additional term $i\delta_{iY}\frac{f_{\omega Y}}{2M_Y}\beta\vec{\alpha}\cdot\vec{\nabla}\omega_0$ in the Dirac equation

$$\left[-i\vec{\alpha}\cdot\vec{\nabla} + \beta M^*(\vec{r}) + V(\vec{r}) - i\delta_{iY}\frac{f_{\omega Y}}{2M_Y}\beta\vec{\alpha}\cdot\vec{\nabla}\omega_0\right]\psi = \varepsilon\psi, \qquad (2.3.1.13)$$

where $\delta_{iY} = 1$ for $i = Y = \Lambda, \Sigma$. The tensor term in the axial model is then given by matrix

$$\frac{f_{\omega Y}}{2M_Y}\begin{bmatrix} 0 & 0 & \partial_z\omega^0 & \left(\partial_{r_\perp} + \frac{\Omega+1/2}{r_\perp}\right)\omega^0 \\ 0 & 0 & \left(\partial_{r_\perp} - \frac{\Omega-1/2}{r_\perp}\right)\omega^0 & -\partial_z\omega^0 \\ -\partial_z\omega^0 & -\left(\partial_{r_\perp} + \frac{\Omega+1/2}{r_\perp}\right)\omega^0 & 0 & 0 \\ \left(\partial_{r_\perp} - \frac{\Omega-1/2}{r_\perp}\right)\omega^0 & \partial_z\omega^0 & 0 & 0 \end{bmatrix}, \qquad (2.3.1.14)$$

which has to be added into equation (2.3.1.9). The Dirac equation (2.3.1.10) after including the tensor interaction acquires the form

$$\begin{pmatrix} A_{\alpha,\alpha'} & B_{\tilde{\alpha},\alpha'} + T_{\tilde{\alpha},\alpha'} \\ B_{\alpha,\tilde{\alpha}'} - T_{\tilde{\alpha},\alpha'} & -C_{\tilde{\alpha},\tilde{\alpha}'} \end{pmatrix}\begin{pmatrix} f_\alpha \\ g_{\tilde{\alpha}} \end{pmatrix} = \varepsilon\begin{pmatrix} f_\alpha \\ -g_{\tilde{\alpha}} \end{pmatrix}, \qquad (2.3.1.15)$$

where $T_{\alpha,\alpha'}$ is given by

$$
\begin{aligned}
T_{\alpha,\alpha'} &= \frac{f_{\omega Y}}{2M_Y}\delta_{m_l,m'_l}\delta_{m_s,m'_s}(-1)^{-\frac{1}{2}+m_s}\int_{-\infty}^{\infty}d\zeta e^{-\zeta^2}H_{n_z}(\zeta)H_{n'_z}(\zeta) \\
&\times\int_0^{\infty}d\eta\,\eta^{|m_l|}e^{-\eta}L_{n_r}^{|m_l|}(\eta)L_{n'_r}^{|m'_l|}(\eta)\left[\partial_z\omega^0\left(b_z\zeta,b_\perp\sqrt{\eta}\right)\right]+ \\
&+\frac{f_{\omega Y}}{2M_Y}\delta_{m_s,m'_s+1}\delta_{m_l,m'_l-1}\int_{-\infty}^{\infty}d\zeta e^{-\zeta^2}H_{n_z}(\zeta)H_{n'_z}(\zeta) \\
&\times\int_0^{\infty}d\eta\,\eta^{|m_l|}e^{-\eta}L_{n_r}^{|m_l|}(\eta)L_{n'_r}^{|m'_l|}(\eta)\left[\left(\partial_{r_\perp}-\frac{\Omega-\frac{1}{2}}{r_\perp}\right)\omega^0\left(b_z\zeta,b_\perp\sqrt{\eta}\right)\right] \\
&\delta_{m_s,m'_s-1}\delta_{m_l,m'_l+1}\int_{-\infty}^{\infty}d\zeta e^{-\zeta^2}H_{n_z}(\zeta)H_{n'_z}(\zeta) \\
&\times\int_0^{\infty}d\eta\,\eta^{|m_l|}e^{-\eta}L_{n_r}^{|m_l|}(\eta)L_{n'_r}^{|m'_l|}(\eta)\left[\left(\partial_{r_\perp}+\frac{\Omega+\frac{1}{2}}{r_\perp}\right)\omega^0\left(b_z\zeta,b_\perp\sqrt{\eta}\right)\right]
\end{aligned}
\qquad (2.3.1.16)
$$

All the functions in this expression are known except ω^0. Thus, to evaluate $T_{\alpha,\alpha'}$ we need to solve the corresponding Klein-Gordon equation for ω^0.

2.3.2 Numerical solution of Klein-Gordon equations

The Klein-Gordon equations in cylindrical coordinates can be expressed as:

$$
\left(-\frac{4}{b_\perp^2}\partial_\eta-\frac{4}{b_\perp^2}\eta\partial_\eta^2-\frac{1}{b_z^2}\partial_\xi^2+m_\phi^2\right)\phi(z,r_\perp)=s_{\phi N}(z,r_\perp)+s_{\phi Y}(z,r_\perp), \qquad (2.3.2.1)
$$

where the notation of the source corresponds to (2.2.19) and the dimensionless coordinates are the same as in equation (2.3.1.6) introduced in previous section.

The solution of the Klein-Gordon equation expanded in a deformed oscillator basis now reads

$$\phi(z,r_\perp)=\frac{1}{b_\perp\sqrt{b_z}}e^{-\xi^2/2}e^{-\eta/2}\sum_{n_z,n_{r_\perp}}\phi_{n_z,n_{r_\perp}}N_{n_z}H_{n_z}(\xi)\sqrt{2}\,L_{n_r}(\eta)\,, \tag{2.3.2.2}$$

where $\phi_{n_z,n_{r_\perp}}$ are the expansion coefficients. Inserting the ansatz into equation (2.3.2.1) and using ortogonality relations, we again obtain a set of inhomogeneous linear equations

$$\sum_{n_z,n_r}^{N_B}H_{n'_z n'_r n_z n_r}\phi_{n_z n_r}=s^{\phi}_{n_z n_r}\,. \tag{2.3.2.3}$$

To solve it for unknown $\phi_{n_z,n_{r_\perp}}$, we first need to evaluate the matrix elements $H_{n'_z n'_r n_z n_r}$. The calculations are presented in appendix B. The result is

$$\begin{aligned}H_{n'_z n'_r n_z n_r}=&\left[\frac{1}{b_\perp^2}\left(2n_{r_\perp}+1\right)+\frac{1}{b_z^2}\left(n_z-\frac{1}{2}\right)+m_\phi^2\right]\delta_{n_z,n'_z}\delta_{n_{r_\perp},n'r_{r_\perp}}-\\&-\frac{1}{b_z^2}\frac{1}{2}\left[\sqrt{n'_z\left(n_z+1\right)}\delta_{n_z+2,n'_z}+\sqrt{n_z\left(n'_z+1\right)}\delta_{n_z-2,n'_z}\right]\delta_{n_{r_\perp},n'_{r_\perp}}+\\&+\frac{1}{b_\perp^2}\left[n'_{r_\perp}\,\delta_{n_{r_\perp}+1,n'_{r_\perp}}+n_{r_\perp}\delta_{n_{r_\perp}-1,n'_{r_\perp}}\right]\delta_{n_z,n'_z}\end{aligned} \tag{2.3.2.4}$$

Since the sources are determined by solution of the Dirac equation, the set of coupled equations has to be solved iteratively until self-consistency is achieved.

3. Parameterizations

As was mentioned above, there are several parameter sets for the RMF model. Four of them, which were used in this work, are listed in Table 2. The first is a linear parameter set proposed by Horowitz and Serot (HS) [25]. The HS parameterization is suitable tool for description of the nuclear density and the rms radius. In this simple model, the nonlinear potential (2.1.13) for σ-meson is not taken into account. This affects mainly the nuclear compressibility, which is too high for the linear HS model. In this work, we focus mostly on the binding energies of nuclei where the difference between linear and nonlinear parameterizations also appears, which will become evident later. The advantage of the linear parameterization is its outstanding numerical stability due to its simplicity (small number of parameters).

The remaining three parameterizations are nonlinear with the potential (2.1.13) which is essential for getting more quantitative description of nuclear properties. The NL1 parameterization introduced by P. G. Reinhard et al. [26] was used in our calculation. However, we encounter problems with numerical stability in some cases, mostly for nuclei with high nuclear densities. The parameter set NL-SH of Sharma et al. [27] describes properties of nuclear matter as well as of finite nuclei reasonably well. In our calculation, it confirmed its good numerical stability. The last parameterization TM2 introduced by Y. Sugahara and H. Toki [19] contains extra nonlinear self-coupling term ω^4 for ω-meson field. The corresponding coupling constant is denoted by c_3. The TM2 model was motivated by the relativistic Brueckner-Hartree-Fock (RBHF) theory of nuclear matter. The results of this model for binding energies and rms radii are in very good agreement with experimental data [19].

All these parameterizations were fitted to the nuclear properties of magic nuclei and the saturation point of nuclear matter. By adding the coupling constants for hyperons, we complete the parameter sets of the RMF model for hypernuclei. The coupling between ω-meson and Λ-hyperon $g_{\omega\Lambda}$ and the constant of the corresponding tensor interaction $f_{\omega Y}$ were taken from quark model [28]. Thus, the adopted values are: $\alpha_{\omega\Lambda} = \frac{g_{\omega\Lambda}}{g_{\omega N}} = 2/3$, $f_{\omega\Lambda} = -1$. The coupling constant $g_{\sigma\Lambda}$ was adjusted to reproduce the ground state binding energy of Λ in the hypernucleus O^{17}_{Λ}, where $B_\Lambda \approx 13$MeV. This gives evidently different values of $g_{\sigma\Lambda}$ for

particular parameter sets. The values of $\alpha_{\sigma\Lambda} = \frac{g_{\sigma\Lambda}}{g_{\sigma N}}$ for corresponding parameterizations under consideration are presented in Table 3.

Finally, the couplings for a Σ-hyperon $\alpha_{\sigma\Sigma} = \frac{g_{\omega\Sigma}}{g_{\omega N}} = 0.544$, $\alpha_{\omega\Sigma} = \frac{g_{\omega\Sigma}}{g_{\omega N}} = 2/3$, $\alpha_{\omega\Sigma} = \frac{g_{\omega\Sigma}}{g_{\omega N}} = 2/3$ were determined from fits to Σ-atom data, for reference see [12].

Table 2: Parameterizations for RMF model used in this work

	HS	NL1	NL-SH	TM2
M (MeV)	939	938	939	938
m_σ (MeV)	520	492.25	526.059	526.443
m_ω (MeV)	783	795.359	783	783
m_ρ (MeV)	770	763	763	770
g_σ	10.47	10.138	10.444	11.4694
g_ω	13.80	13.285	12.945	14.6377
g_ρ	8.07	9.051	8.766	8.3566
g_2 (fm^{-1})	0	-12.172	-6.9099	4.444
g_3	0	-36.265	-15.8337	4.6076
c_3	0	0	0	84.5318

Table 3: Couplings for Λ hyperon interaction: $\alpha_{i\Lambda} = \frac{g_{i\Lambda}}{g_{iN}}$, where i=σ, ω.

	HS	NL1	NL-SH	TM2
$\alpha_{\sigma\Lambda}$	0.623	0.618	0.618	0.621
$\alpha_{\underline{\omega\Lambda}}$	2/3	2/3	2/3	2/3
$f_{\omega\Lambda}$	-1	-1	-1	-1

4. Results and discussion

Hypernuclear properties were studied for isotopes of Be, C, O and Ne with even number of neutrons. The range of calculated isotopes for a particular chemical element approximately corresponds to the known measured isotopes of the considered chemical elements. Before we proceed to hypernuclear calculations, we will test our nuclear model on exotic nuclei without hyperons. First, we will compare the spherical and axial approaches. Second, we will compare the applied RMF parameter sets. The binding energies per particle E/A for Be, C, O and Ne calculated in the spherical and axial code are compared with experimental values [29], [30] in figures 1a, 1b, 1c, 1d respectively.

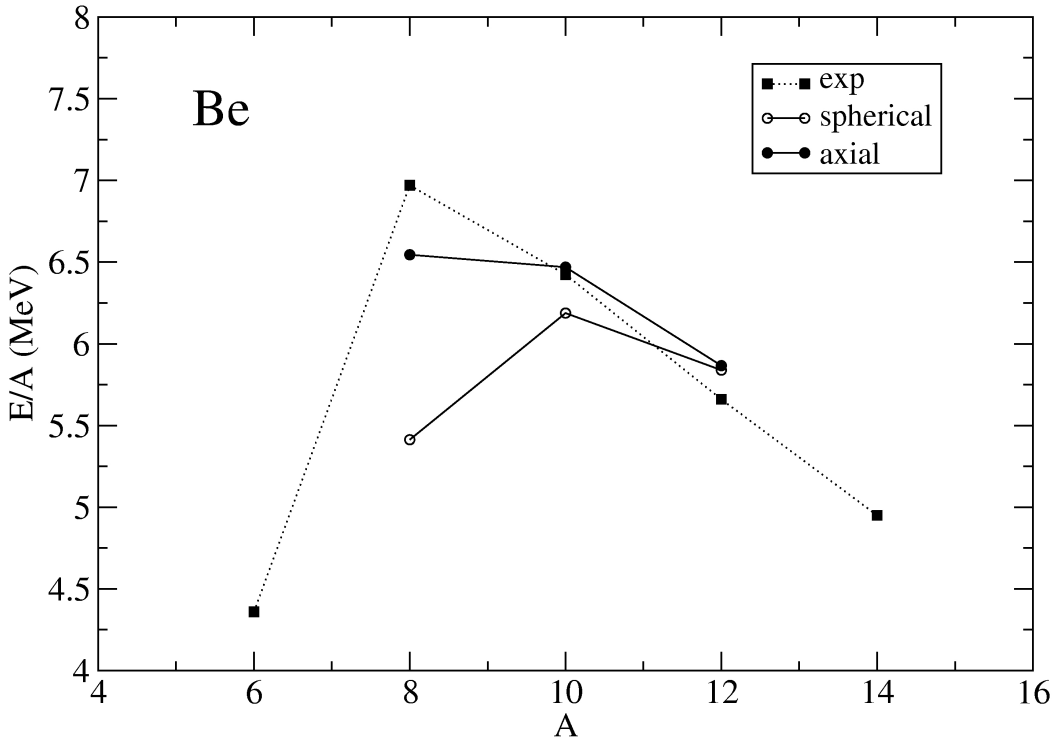

Fig.1a: Binding energy E/A in Be isotopes as function of A. Results for spherical and axial calculations within the nonlinear RMF model NL-SH are compared with experimental values.

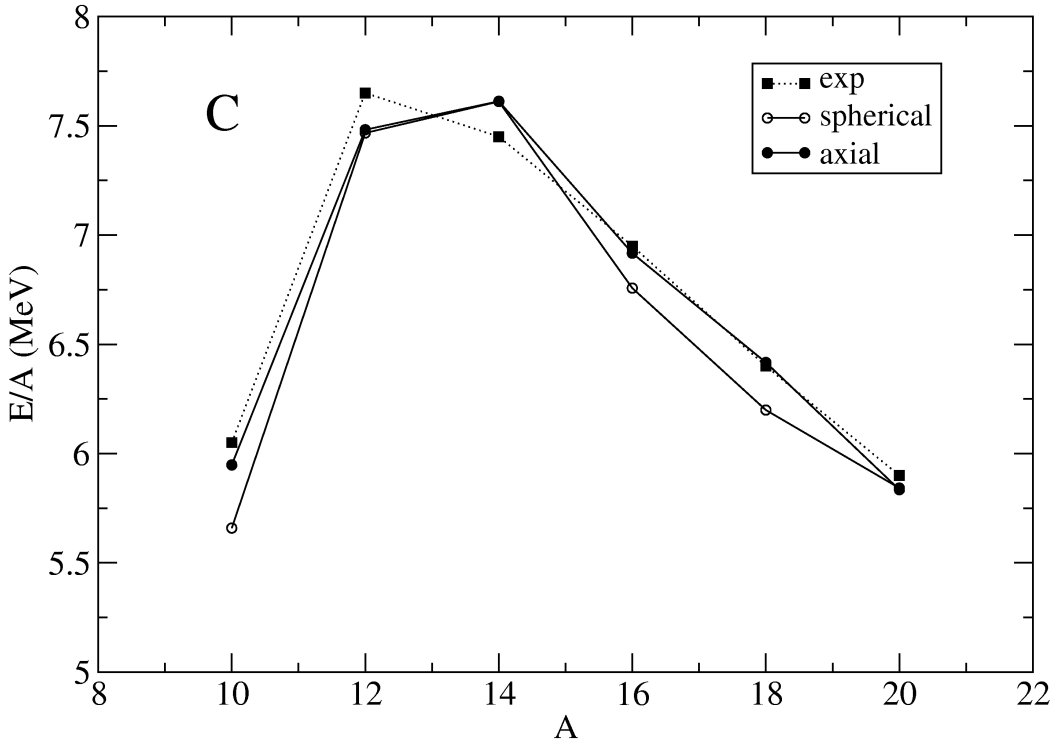

Fig. 1b: Binding energy E/A in C isotopes as function of A. Results for spherical and axial calculations within the nonlinear RMF model NL-SH are compared with experimental values.

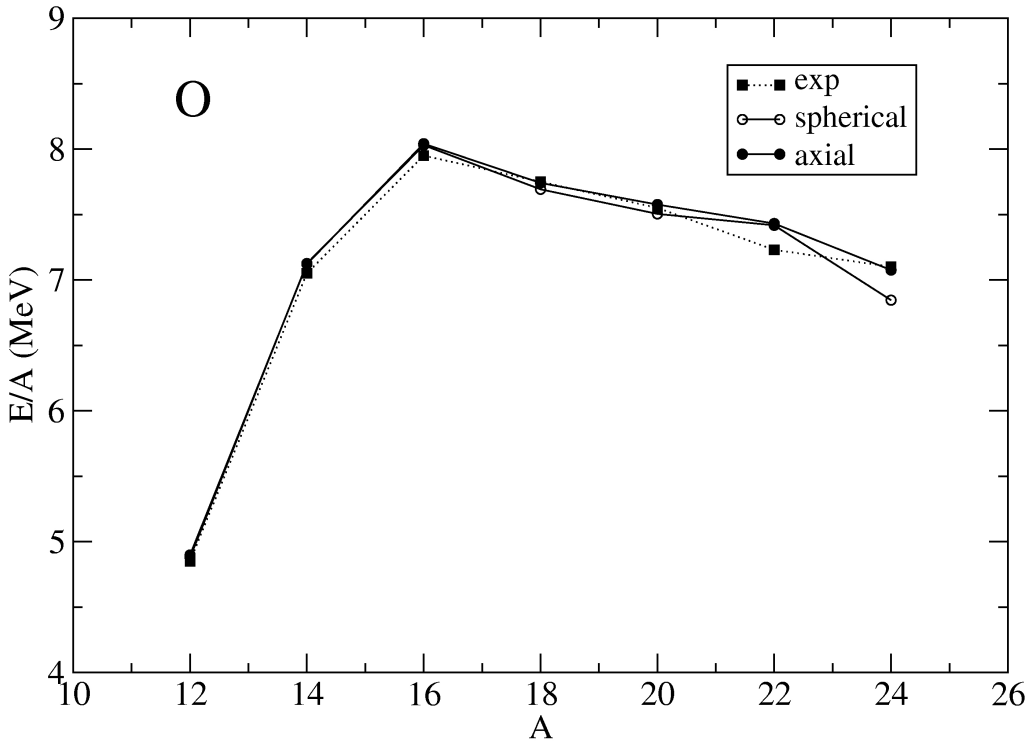

Fig 1c: Binding energy E/A in O isotopes as function of A. Results for spherical and axial calculations within the nonlinear RMF model NL-SH are compared with experimental values.

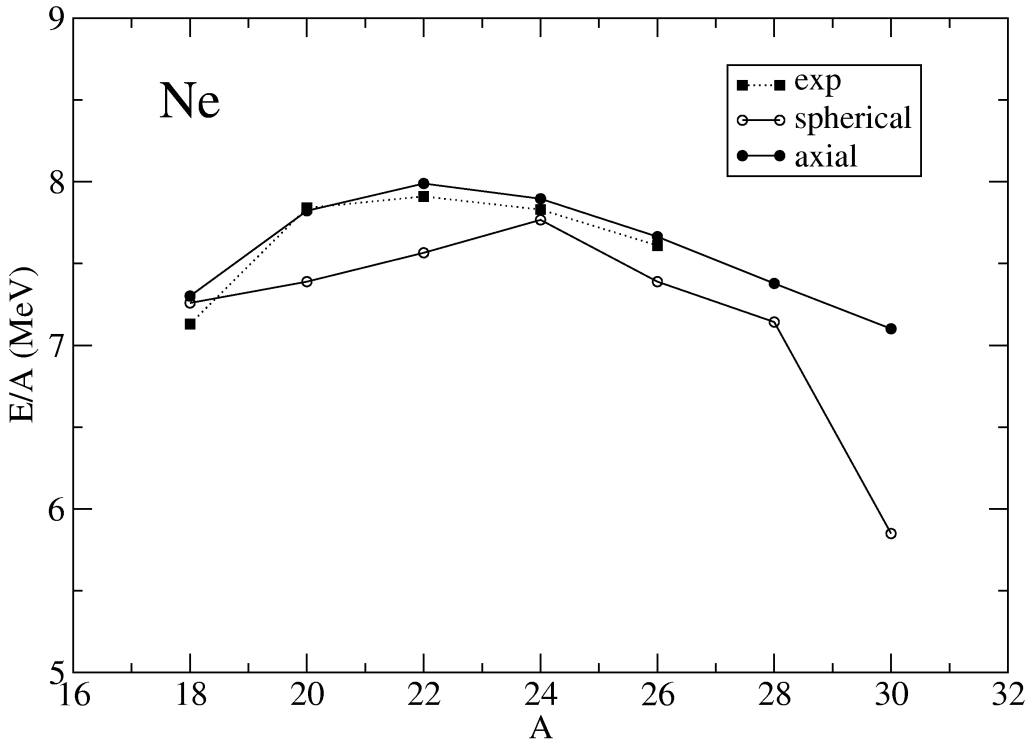

Fig.1d: Binding energy E/A in Ne isotopes as function of A. Results for spherical and axial calculations within the nonlinear RMF model NL-SH are compared with experimental values.

The results for the isotopes of carbon (with exception for ^{14}C), oxygen and neon are in good agreement with experimental values, particularly for oxygen. On the contrary, the results for beryllium are significantly different from experiment. Moreover, for Be^{8} and Be^{12}, we obtained that the last proton is not coupled to the nucleus any more. The failure might indicate that Be isotopes are too light systems to be described by a mean field approximation. Presented figures clearly show that the results for the axial case are always in better agreement with the experimental values than the spherical ones. Therefore, we will use the axial model in the following.

Next, we focus on comparison and applicability of used parameterizations. The comparison of the considered parameterizations for oxygen isotopes is in figure 2. From our calculations it follows that the linear model HS gives much lower binding energies E/A (by about 2.5 MeV) than the nonlinear models. The results for the nonlinear parameterizations NL1, TM2 and NL-SH are almost identical with only marginal differences. In comparison with experiment, the nonlinear models give considerably better results for nuclear binding energies than the linear HS model. On the other hand, during calculations problems with

convergence of the iterative procedure occurred for some isotopes in the case of nonlinear parameterizations NL1 and TM2 (the problem of the stability of the nonlinear models is discussed in ref.[18]). The most stable parameterization from this point of view is the linear HS model. The NL-SH parameterization appears to be more stable than NL1 and TM2 so we will present mainly results for the NL-SH model in the following figures.

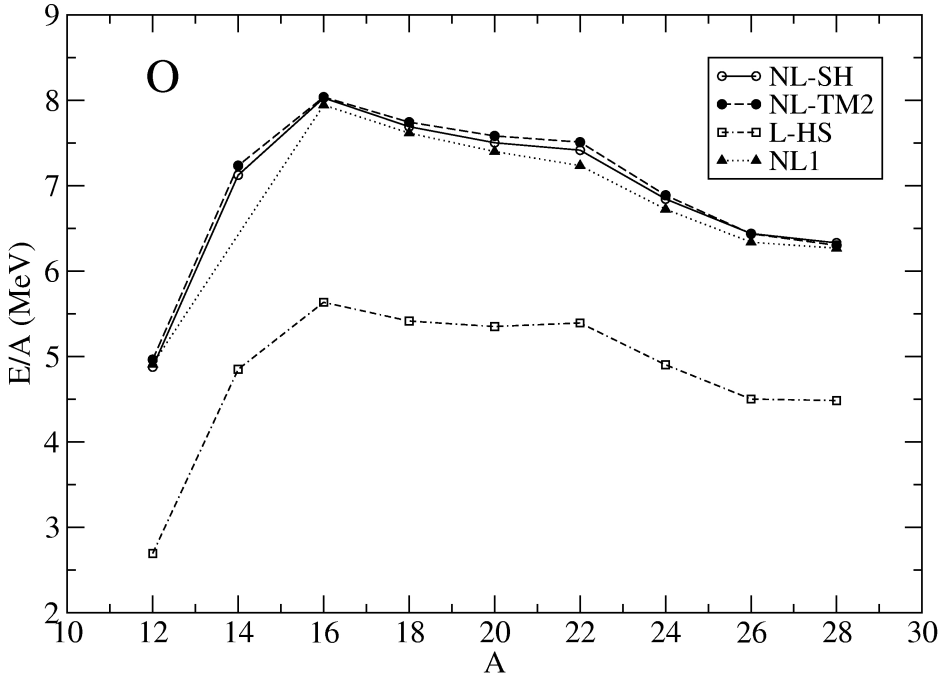

Fig. 2: Binding energy E/A as function of A for oxygen isotopes calculated in axial code for different RMF parameterizations. The missing value of C^{14} for NL1 parameterization is due to its convergence problems.

4.1. Exotic Λ hypernuclei

In this section, we will present results of the study of the Λ-hyperon in the following order: the influence of the Λ hyperon on the nuclear binding energy per particle, the shrinkage of a nucleus in the presence of the Λ hyperon, contribution of the tensor interaction to the spin orbit splitting.

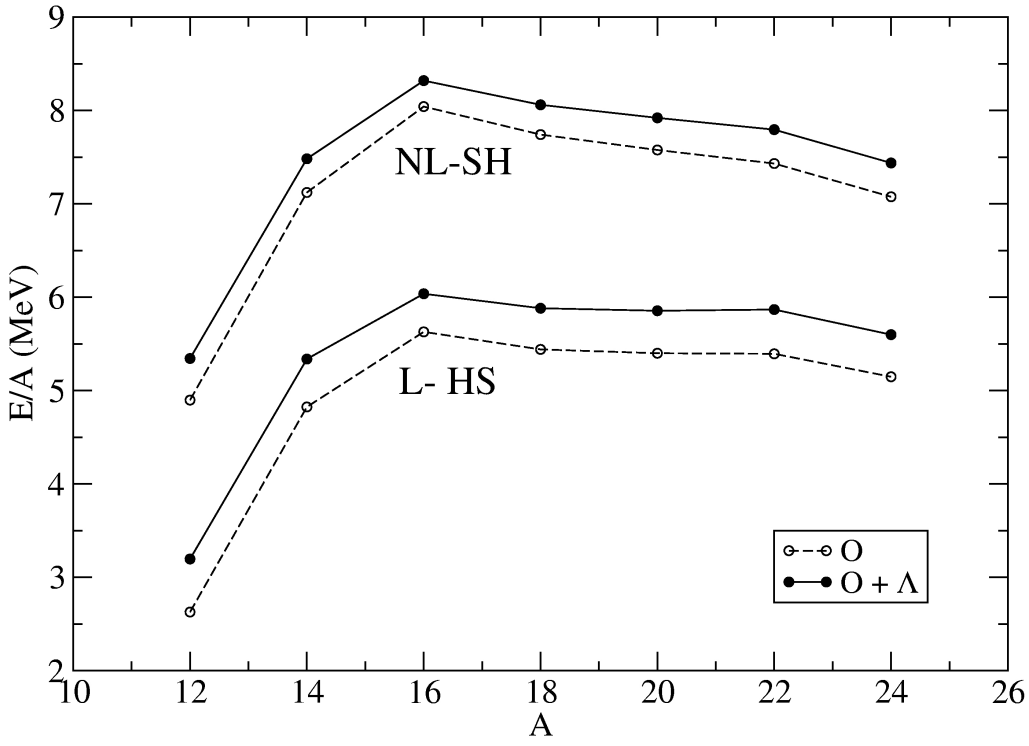

Fig. 3: Binding energy E/A as function of A for O isotopes and O+Λ systems. Calculations were done for linear model and nonlinear model NL-SH.

Figure 3 demonstrates the influence of the Λ-hyperon on the nuclear core in oxygen isotopes. Since the binding energy per particle is shifted upward, it is obvious that the presence of Λ in nucleus leads to more coupled system. This effect is caused by the strangeness of the Λ-particle. Due to the nonzero strangeness, the Λ-particle is distinguishable from the rest of the nucleons and therefore it is allowed to occupy the 1s state. Moreover, since the Λ-nuclear interaction is attractive, Λ hyperon acts as a “glue” in the nuclear system.

It is interesting that the changes of the binding energy per particle E/A in consequence of the presence of Λ are almost constant for the considered isotopes. Moreover, the linear and nonlinear model predicts a similar value, approximately 0.5 MeV for the shift in E/A due to Λ.

The fact that the presence of the Λ-particle leads to more bound nuclear system manifests itself also in the change of the size of the nuclear system. Although there is one more particle in the nucleus, the root mean square (rms) radius is smaller due to the stronger binding caused by the Λ hyperon. This shrinkage has already been confirmed experimentally in KEK, Japan [31]. The comparison of the rms radii for ordinary exotic nuclei and corresponding hypernuclei is presented in figure 4.

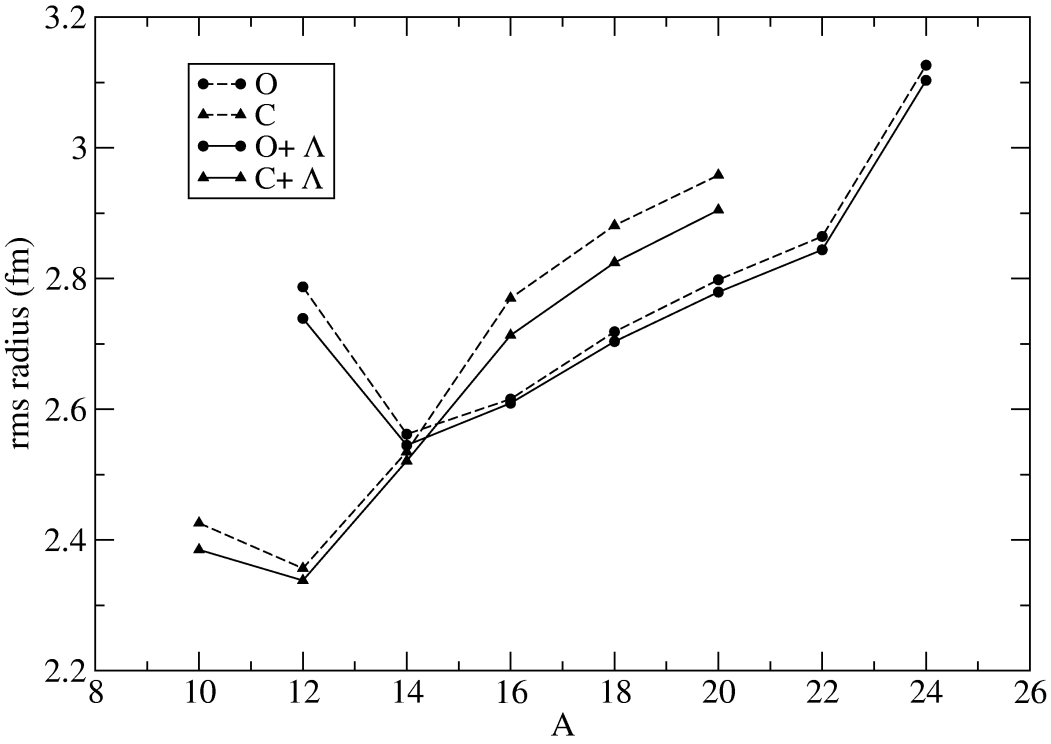

Fig. 4: The rms radius of C and O isotopes, and C+Λ, O+Λ system as function of A.

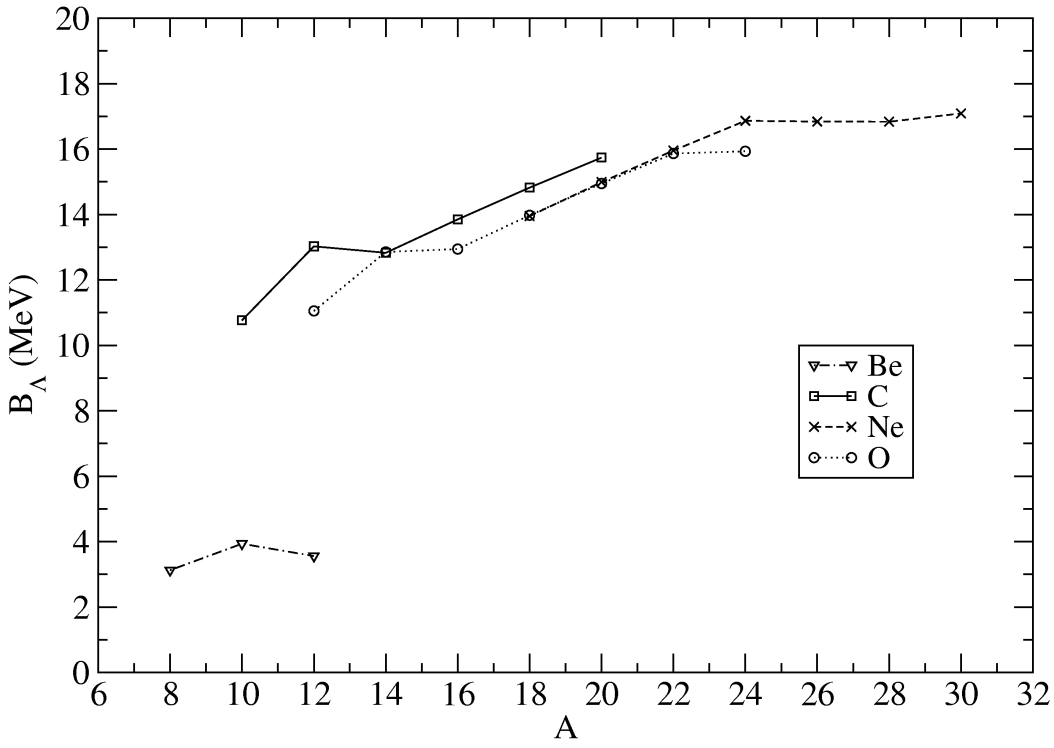

Fig. 5: The Λ binding energy B_Λ in Be, C, O and Ne isotopes as function for A.

In figure 5, we present the results of the calculation of the Λ binding energies. There can be seen a growing trend for C, O and Ne hypernuclei in the figure, while the binding energy per particle decreases in corresponding neutron rich isotopes (see figures 1a to 1d). The behavior is not unexpected. The Λ particle always occupies the lowest s state, while the binding energy E/A acquires also contributions from the weekly bound neutrons from the outer shells.

By introducing the tensor coupling into the model, we are able to describe simultaneously the large spin-orbit splitting for nucleons and the small spin-orbit splitting for the Λ hyperon. It is obvious from figures 6 and 7 that the tensor interaction decreases the energy of the s1/2 and p3/2 states and on the contrary, it increases the energy of the p1/2 state. As a result this leads to sizeable reduction of the spin orbit splitting. All the presented models predict reduction of the spin-orbit splitting du to the tensor coupling to about 1/3 of the original value. The new value is ≈ 0.5 MeV, which is in agreement with experiment. It is worth mentioning that the introduction of the ω-meson tensor coupling influences little the "bulk" properties of hypernuclei, such as the total binding energy, the rms radius or the distribution of matter.

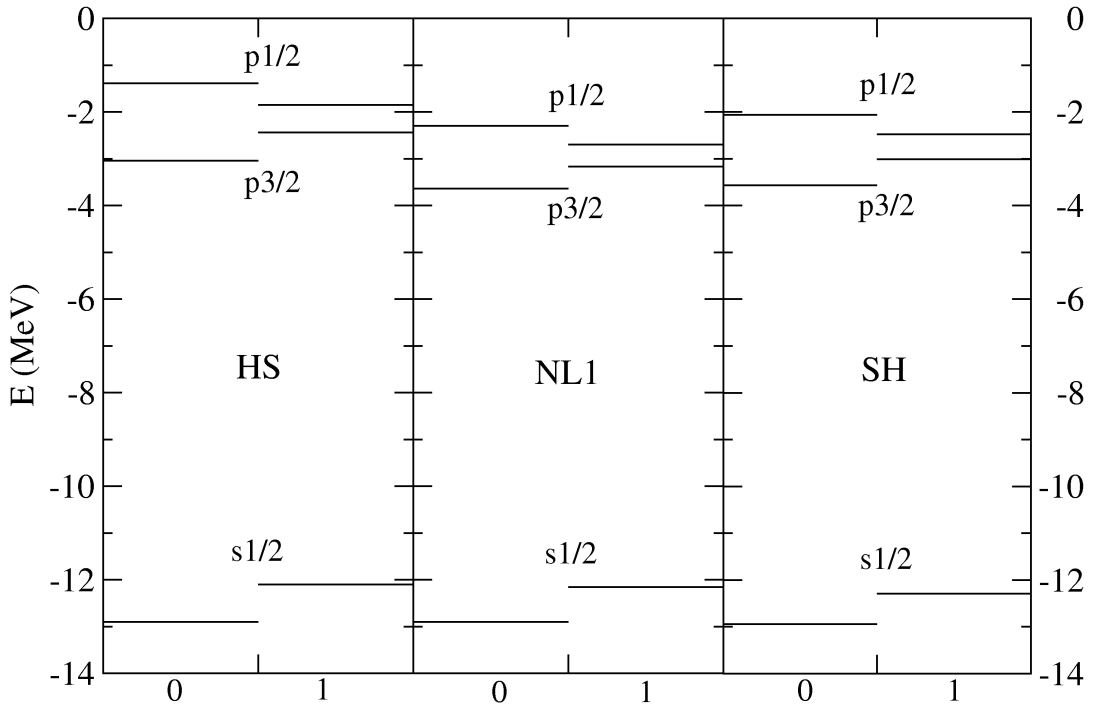

Fig. 6: Effect of the tensor coupling on the position of the hyperon single particle level in ${}^{17}_{\Lambda}\mathrm{O}$. Results of the parameterizations L-HS, NL1, NL-SH are compared, 0 and 1 denotes calculations without and with the tensor coupling term respectively.

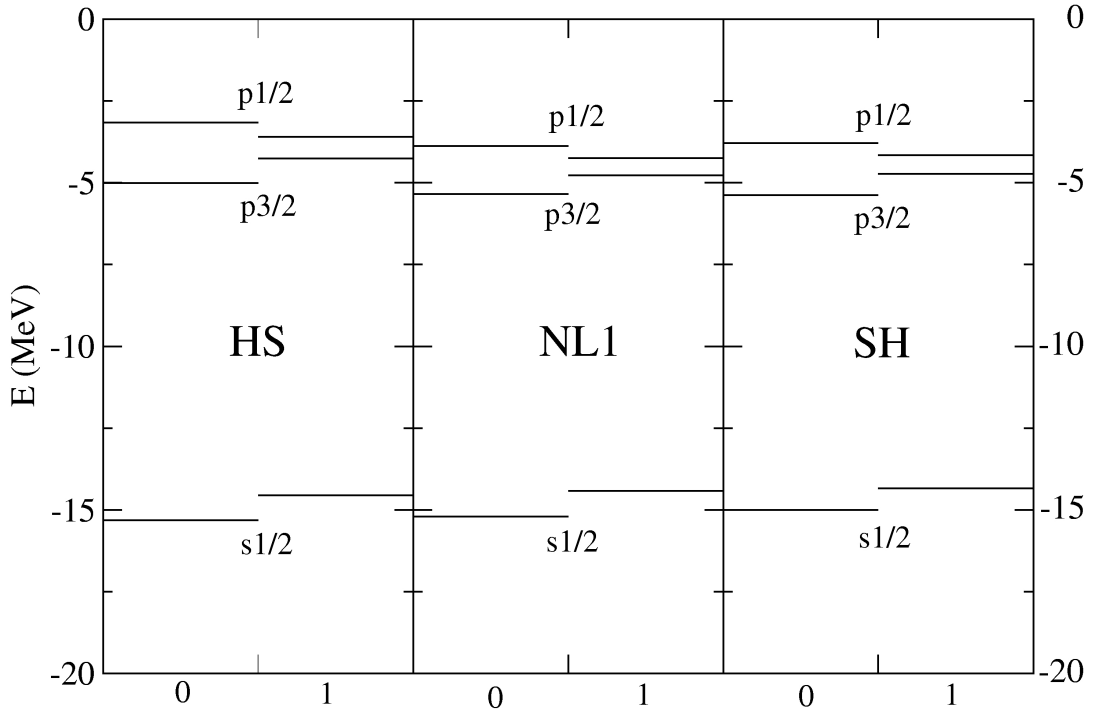

Fig. 7: Effect of the tensor coupling on the position of the hyperon single particle level in ${}^{17}_{\Lambda}\mathrm{Ne}$. Results of the parameterizations L-HS, NL1, NL-SH are compared, 0 and 1 denotes calculations without and with the tensor coupling term respectively.

4.2. Exotic Σ hypernuclei

This section is devoted to the calculation of the binding energies of nuclear systems with a Σ hyperon. As was mentioned in introduction, the Σ hypernuclear bound state has not been observed, with exception for ${}^{4}_{\Sigma}\mathrm{He}$ [10]. The study of the Σ-nucleus interaction in Σ atoms predicts no Σ^+ hypernuclear bound states [12]. Although the Σ-nucleus isovector potential cancels partly (for charged $\Sigma^{\pm}$) the Coulomb potential, the Coulomb and the isoscalar repulsive potentials for Σ^+ overcome the attraction due to the isovector potential (ρ-meson). For Σ^-, the calculations in [12] predict possible bound states for high Z nuclear cores.

It is to be noted that calculations of exotic Σ hypernuclei have not been performed yet. In this work, we focus on a search for bound states of the Σ hyperon in above mentioned isotopes Be, C, O and Ne. Since the central Σ potential is repulsive, the Coulomb and isovector interactions and their interplay are crucial for a Σ hyperon to be bound in a nucleus. Consequently, it is obvious that Σ^0 bound states need not be considered.

Our calculation confirmed that no Σ^+ bound states exist in the studied isotopes. For Σ^-, we obtained several bound states in the mentioned isotopes. The calculated values of the binding energies are presented in Table 4. The binding energies acquire small values in the range of units of MeV. The attractive Coulomb interaction is responsible for the binding of the Σ^- hyperon in a nucleus (in most cases). It is to be noted that the Σ^- states acquire a finite width of the order of tens Mev due to the conversion $\Sigma^- p \rightarrow \Lambda n$. Since the RMF approach does not address directly the imaginary part of the potential due to the absorption, we have not considered the width of the Σ states in this work.

Table 4: Binding energy B_Σ for Σ hyperon, sign minus (plus) corresponds to (un)bound states.

	^{8}Be	^{12}Be	^{10}C	^{12}C	^{20}C	^{12}O	^{16}O	^{22}O	^{18}Ne	^{20}Ne	^{30}Ne
B_Σ(MeV)	-1.02	-0.58	-2.97	-1.74	-0.85	-3.20	-2.64	-1.37	+1,64	+1,73	-1,58

5. Conclusions

We performed self-consistent calculations of Λ and Σ exotic hypernuclei within the framework of the relativistic mean-field theory. We adopted the axial symmetry approach for ordinary nuclei from [23] and extended it to the hypernuclear region, including the tensor interaction between the ω-meson and a hyperon. To compare the axially symmetric case with the spherical one we made calculations of Be, C, O and Ne isotopes also in the spherical code and compared both cases with the experimental data. The results confirmed that the axially deformed code gives values of the binding energies in better agreement with experiment than the spherical one. In reference [23], errors were found in equations of motion for the spherically symmetric case (for more see the section 2.2 and 2.3.1).

Since the RMF theory as a phenomenological model depends on a set of parameters, we applied four most widely used parameterizations. The results for each of them manifest that the nonlinear parameterizations are much suitable for calculations of binding energies than the linear one. On the other hand, the linear parameterization is the best as regards numerical stability. Taking into account both of these points, we conclude that from the considered parameterizations the most appropriate is NL-SH model.

For the above isotopes of Be, C, O and Ne, we studied the influence of Λ hyperon mostly on the bulk properties of nuclear systems. We calculated the binding energy of hypernuclei in the ground state and confirmed that the presence of the Λ hyperon shifts the binding energy of a nucleus and makes the nuclear system more bound. Moreover, we observed that the shifts of the binding energy per particle caused by the Λ hyperon are almost identical for all isotopes of the particular chemical element. Thus, the Λ hyperon contribution to the total nuclear binding is almost independent of the number of neutrons. The binding energy of the hyperon itself was studied as function of A for above mentioned isotopes. We obtained, in general, increasing function of nucleons, which one can expect considering previous results.

Embedding the Λ hyperon into a nucleus obviously affects also its size, characterized by a root mean square radius. The evaluations of the rms radii give smaller values for the nuclei with the Λ hyperon than for the ordinary ones, which is in agreement with experiment [31]. The reason of this result lies in the higher binding energies for hypernuclei and the glue-like character of the Λ hyperon in a nuclear system.

Σ hypernuclei were the next studied hypernuclear systems. We analyzed the possible existence of bound Σ hypernuclear states. This topic was already discussed in [12] in connection with the Coulomb and isovector interaction involved in the Lagrangian, which could cause the binding of a Σ hyperon. Our particular calculation confirmed previous estimates for Σ^+ as we found no bound states in Be, C, O and Ne isotopes. However, we obtained some weekly bound states for the Σ^- hyperon. In this case, the Coulomb interaction is the dominating force.

In the end, it is to be noted that our calculations of Λ and Σ exotic hypernuclei are to be considered only estimates at present. For most of the obtained results, there are no experimental data available yet. Nevertheless, the experimental study of exotic hypernuclei currently takes place in KEK, JLab and FINUDA laboratories and, therefore, the data are expected to come soon.

Appendix A

The ortogonality relations of the harmonic oscillator eigenstates are

$$\left\langle \Phi_\alpha \middle| \Phi_{\alpha'} \right\rangle = \sum_{s,s'=1}^{2} \int_0^{2\pi} \int_{-\infty}^{\infty} \int_{-\infty}^{\infty} \Phi_\alpha \Phi^+_{\alpha'} r\, dr\, dz\, d\varphi = \sum_{s,s'=1}^{2} \int_0^{2\pi} \int_{-\infty}^{\infty} \int_{-\infty}^{\infty} \Phi_\alpha \Phi^+_{\alpha'} \frac{1}{2} b_z b_\perp^2\, d\eta\, d\xi\, d\varphi =$$

$$= \frac{1}{2} b_z b_\perp^2 \sum_{s,s'=1}^{2} \int_{-\infty}^{\infty} d\xi \frac{N_{n_z} N_{n'_z}}{b_z} e^{-\xi^2} H_{n_z}(\xi) H_{n'_z}(\xi) \times \int_{-\infty}^{\infty} d\eta \frac{N^{m_l}_{n_{r_\perp}} N^{m'_l}_{n'_{r_\perp}}}{b_\perp^2} 2\eta^{\frac{|m_l|+|m'_l|}{2}} e^{-\eta} L^{|m_l|}_{n_{r_\perp}}(\eta) L^{|m'_l|}_{n'_{r_\perp}}(\eta)$$

$$\times \int_{-\infty}^{\infty} d\varphi \frac{1}{2\pi} e^{i(m_l - m'_l)\varphi} \chi_{m_l}(s) \chi_{m'_s}(s) =$$

$$= \sum_{s,s'=1}^{2} \chi_{m_l}(s) \chi_{m'_s}(s) \int_{-\infty}^{\infty} d\xi\, N_{n_z} N_{n'_z} e^{-\xi^2} H_{n_z}(\xi) H_{n'_z}(\xi) \times \int_0^{\infty} d\eta\, N^{m_l}_{n_{r_\perp}} N^{m'_l}_{n'_{r_\perp}} \eta^{\frac{|m_l|+|m'_l|}{2}} e^{-\eta} L^{|m_l|}_{n_{r_\perp}}(\eta) L^{|m'_l|}_{n'_{r_\perp}} \times \delta_{m_l, m'_l} =$$

$$= \delta_{m_s, m'_s} \delta_{n_z, n'_z} \delta_{n_{r_\perp}, n'_{r_\perp}} \delta_{m_l, m'_l} \tag{A1}$$

where we use the ortogonality relations for Hermite and Laguerre polynomials [24]

$$\int_{-\infty}^{\infty} e^{-x^2} H_n(x) H_m(x) = 2^n n! \sqrt{\pi} \delta_{n,m}$$

$$\int_{-\infty}^{\infty} e^{-\eta} \eta^\alpha L^\alpha_n(x) L^\alpha_m(x) = \frac{\Gamma(\alpha + n + 1)}{n!} \delta_{n,m} \tag{A2}$$

The computation of $B_{\alpha,\alpha'}$.

First, we introduce some useful relations for the evaluation of the derivatives of the eigenfunctions Φ of an axially symmetric harmonic oscillator (2.3.1.4)

$$\partial_z \phi_{n_z}(z) = \frac{N_z}{b_z^{3/2}} \tilde{H}_{n_z}(\xi) e^{-\xi^2/2}$$

$$\partial_r \phi^{m_l}_{n_r}(r_\perp) = \frac{N^{m_l}_{n_{r_\perp}}}{b_\perp^2} \sqrt{2} \eta^{(m_l - 1)/2} \tilde{L}^{m_l}_{n_{r_\perp}}(\eta) e^{-\eta/2} \tag{A3}$$

where

$$\tilde{H}_{n_z}(\xi) = \xi H_{n_z}(\xi) - H_{n_z+1}(\xi)$$

$$\tilde{L}^{m_l}_{n_{r_\perp}}(\eta) = \left(2n_{r_\perp} + m_l - \eta\right) L^{m_l}_{n_{r_\perp}}(\eta) - 2\left(n_{r_\perp} + m_l\right) L^{m_l}_{n_{rj}-1}(\eta). \tag{A4}$$

The term in $B_{\alpha,\alpha'}$ with the derivatives ∂_z reads

$$\left\langle \Phi_{\alpha'} \left| \partial_z \Phi_\alpha \right\rangle = \frac{1}{2} b_z b_\perp^2 \sum_{s,s'=1}^{2} \int_0^{2\pi} \int_{-\infty}^{\infty} \int_0^{\infty} d\eta\, d\xi\, d\varphi\, \phi_{n'_z}(z) \phi_{n'_{r_\perp}}^{m'_l}(r_\perp) \frac{1}{\sqrt{2\pi}} e^{-im'_l\varphi} \chi_{m'_s}(s') \times \right.$$

$$\left. \times \left(\partial_z \phi_{n_z}(z)\right) \phi_{n_{r_\perp}}^{m_l}(r) \frac{1}{\sqrt{2\pi}} e^{im_l\varphi} \chi_{m_s}(s) = \delta_{n_{r_\perp},n'_{r_\perp}} \delta_{m_l,m'_l} \delta_{m_s,m'_s} \int_{-\infty}^{\infty} d\xi\, \phi_{n'_z} \partial_\xi \phi_{n_z} = \right.$$

$$\delta_{n_{r_\perp},n'_{r_\perp}} \delta_{m_l,m'_l} \delta_{m_s,m'_s} \frac{N_{n_z} N_{n'_z}}{b_z} \int_{-\infty}^{\infty} d\xi\, H_{n'_z}(\xi) e^{-\xi^2/2} \partial_\xi \left(H_{n_z}(\xi) e^{-\xi^2/2} \right) =$$

$$= \delta_{n_{r_\perp},n'_{r_\perp}} \delta_{m_l,m'_l} \delta_{m_s,m'_s} \frac{1}{b_z} \frac{1}{\sqrt{\sqrt{\pi} 2^{n_z} n_z!} \sqrt{\sqrt{\pi} 2^{n'_z} n'_z!}} \left(-\sqrt{\pi} \right) \left(2^{n_z} n'_z!\, \delta_{n'_z,n_z+1} - 2^{n'_z} n_z!\, \delta_{n'_z,n_z-1} \right) =$$

$$= \delta_{n_{r_\perp},n'_{r_\perp}} \delta_{m_l,m'_l} \delta_{m_s,m'_s} \frac{1}{b_z} \left(\sqrt{\frac{2^{n_z}}{2^{n'_z}} \frac{n'_z!}{n_z!}} \delta_{n'_z,n_z+1} - \sqrt{\frac{2^{n'_z}}{2^{n_z}} \frac{n_z!}{n'_z!}} \delta_{n'_z,n_z-1} \right) =$$

$$\delta_{n_{r_\perp},n'_{r_\perp}} \delta_{m_l,m'_l} \delta_{m_s,m'_s} \frac{1}{b_z} \left(\sqrt{\frac{n'_z}{2}} \delta_{n'_z,n_z+1} - \sqrt{\frac{n_z}{2}} \delta_{n'_z,n_z-1} \right) \tag{A5}$$

Here, the relation

$$\int_{-\infty}^{\infty} e^{-x^2/2} H_n(x) \frac{d}{dx} \left(e^{-x^2/2} H_n(x) \right) = -\sqrt{\pi} \left(2^m n!\, \delta_{n,m+1} - 2^{nj} m!\, \delta_{n,m-1} \right). \tag{A6}$$

for Hermite polynomials was used [24].

The term corresponding to $\left(\partial_r + (-1)^{m_s+1/2} \frac{\Omega + (-1)^{m_s+1/2} 1/2}{r} \right)$ can be written as

$$\left\langle \Phi_{\alpha'} \left| \partial_{r_\perp} + (-1)^{m_s+1/2} \frac{\Omega + (-1)^{m_s+1/2} 1/2}{r_\perp} \right| \Phi_\alpha \right\rangle \frac{1}{2} b_z b_\perp^2 \sum_{s,s'=1}^{2} \int_0^{2\pi} \int_{-\infty}^{\infty} \int_0^{\infty} d\eta\, d\xi\, d\varphi\, \phi_{n'_z}(z) \phi_{n'_{r_\perp}}^{m'_l}(r_\perp) \frac{1}{\sqrt{2\pi}} e^{-im'_l\varphi} \chi_{m'_s}(s') \times$$

$$\times \phi_{n_z}(z) \left(\partial_{r_\perp} + (-1)^{m_s+1/2} \frac{\Omega + (-1)^{m_s+1/2} 1/2}{r_\perp} \right) \phi_{n_{r_\perp}}^{m_l}(r_\perp) \frac{1}{\sqrt{2\pi}} e^{im_l\varphi} \chi_{m_s}(s) =$$

$$= \frac{1}{2} b_\perp^2 \delta_{n_z,n'_z} \sum_{s,s'} \int_0^{2\pi} e^{i(m_l-m'_l)\varphi} \chi_{m'_s}(s') \chi_{m_s}(s) d\varphi \int_0^{\infty} \phi_{n'_{r_\perp}}^{m'_l}(r_\perp) \left(\partial_{r_\perp} + (-1)^{m_s+1/2} \frac{m_l}{r_\perp} \right) \phi_{n_{r_\perp}}^{m_l}(r_\perp) d\eta =$$

$$= \frac{1}{2} b_\perp^2 \delta_{n_z, n'_z} \frac{N_{n_{r_\perp}}^{m_l} N_{n'_{r_\perp}}^{m'_l}}{b_\perp^2 b_\perp} \sqrt{2}\sqrt{2} \Bigg\{ \delta_{m_s, m'_s+1} \delta_{m_l, m'_l-1} \int_0^\infty d\eta\, e^{-\eta/2} \eta^{m'_l/2} L_{n'_{r_\perp}}^{m'_l} \left(\eta^{(m_l-1)/2} \tilde{L}_{n_{r_\perp}}^{m_l} - \frac{1}{\eta} m_l \eta^{m_l/2} L_{n_{r_\perp}}^{m_l} \right) e^{-\eta/2} +$$

$$\delta_{m_s, m'_s-1} \delta_{m_l, m'_l+1} \int_0^\infty d\eta\, e^{-\eta/2} \eta^{m'_l/2} L_{n'_{r_\perp}}^{m'_l} \left(\eta^{(m_l-1)/2} \tilde{L}_{n_{r_\perp}}^{m_l} + \frac{1}{\eta} m_l \eta^{m_l/2} L_{n_{r_\perp}}^{m_l} \right) e^{-\eta/2} \Bigg\} =$$

$$= \delta_{n_z, n'_z} \frac{N_{n_{r_\perp}}^{m_l} N_{n'_{r_\perp}}^{m'_l}}{b_\perp} \Bigg\{ \delta_{m_s, m'_s+1} \delta_{m_l, m'_l-1} \int_0^\infty d\eta\, e^{-\eta} \eta^{m_l} L_{n'_{r_\perp}}^{m'_l} \left(\tilde{L}_{n_{r_\perp}}^{m_l} - m_l L_{n_{r_\perp}}^{m_l} \right) +$$

$$\delta_{m_s, m'_s-1} \delta_{m_l, m'_l+1} \int_0^\infty d\eta\, e^{-\eta} \eta^{m_l-1} L_{n'_{r_\perp}}^{m'_l} \left(\tilde{L}_{n_{r_\perp}}^{m_l} + m_l L_{n_{r_\perp}}^{m_l} \right) \Bigg\} \tag{A7}$$

where $\Omega = m_l + m_s$.

Appendix B

The matrix elements $H_{n'_z n'_r n_z n_r}$ from equation (2.3.2.3).

The Klein-Gordon equation (2.3.2.1) reads

$$\left(-\frac{4}{b_\perp^2}\partial_\eta - \frac{4}{b_\perp^2}\eta\partial_\eta^2 - \frac{1}{b_z^2}\partial_\xi^2 + m_\phi^2\right)\phi(z,r_\perp) = s_{\phi N}(z,r_\perp) + s_{\phi Y}(z,r_\perp). \tag{B1}$$

First, we evaluate the terms corresponding to derivatives with respect to η.

$$\begin{aligned}
&\partial_\eta\left(e^{-\eta/2}L_{n_{r_\perp}}(\eta)\right) = -\frac{1}{2}e^{-\eta/2}L_{n_{r_\perp}} + e^{-\eta/2}\partial_\eta L_{n_{r_\perp}} \\
&\eta\partial_\eta^2\left(e^{-\eta/2}L_{n_{r_\perp}}(\eta)\right) = \eta\partial_\eta\left(-\frac{1}{2}e^{-\eta/2}L_{n_{r_\perp}} + e^{-\eta/2}\partial_\eta L_{n_{r_\perp}}\right) = \\
&= \eta\left(\frac{1}{4}e^{-\eta/2}L_{n_{r_\perp}} - \frac{1}{2}e^{-\eta/2}\partial_\eta L_{n_{r_\perp}} - \frac{1}{2}e^{-\eta/2}\partial_\eta L_{n_{r_\perp}} + e^{-\eta/2}\partial_\eta^2 L_{n_{r_\perp}}\right) = \eta e^{-\eta/2}\left(\frac{1}{4}L_{n_{r_\perp}} - \partial_\eta L_{n_{r_\perp}} + \partial_\eta^2 L_{n_{r_\perp}}\right).
\end{aligned} \tag{B2}$$

This leads to

$$\begin{aligned}
&\left(4\partial_\eta + 4\eta\partial_\eta^2\right)\left(e^{-\eta/2}L_{n_{r_\perp}}(\eta)\right) = e^{-\eta/2}\left(-2L_{n_{r_\perp}} + 4\partial_\eta L_{n_{r_\perp}} + \eta L_{n_{r_\perp}} - 4\eta\partial_\eta L_{n_{r_\perp}} + 4\eta\partial_\eta^2 L_{n_{r_\perp}}\right) = \\
&= e^{-\eta/2}\left[(\eta-2)L_{n_{r_\perp}} + (4-4\eta)\partial_\eta L_{n_{r_\perp}} + 4\eta\partial_\eta^2 L_{n_{r_\perp}}\right]
\end{aligned} \tag{B3}$$

Using relations for Laguerre polynomials [24]

$$\frac{d}{dx}L_n(x) = \frac{n}{x}\left[L_n(x) - L_{n-1}(x)\right] \text{ or differently } \frac{d^2}{dx^2}L_n(x) = \frac{n(n-1)}{x^2}\left[L_n(x) - 2L_{n_{r_\perp}-1} + L_{n+2}(x)\right], \tag{B4}$$

we obtain from relation (B3)

$$e^{-\eta/2}\left[(\eta-2)L_{n_{r_\perp}}+4(1-\eta)\frac{n}{\eta}\left(L_{n_{r_\perp}}-L_{n_{r_\perp}-1}\right)+4\eta\frac{n(n-1)}{\eta^2}\left(L_{n_{r_\perp}}-2L_{n_{r_\perp}-1}+L_{n_{r_\perp}-2}\right)\right]=$$
$$e^{-\eta/2}\left[\left(\eta-2+\frac{4n}{\eta}-4n+4\frac{n(n-1)}{\eta}\right)L_{n_{r_\perp}}+\left(-\frac{4n}{\eta}+4n-8\frac{n(n-1)}{\eta}\right)L_{n_{r_\perp}-1}+4\frac{n(n-1)}{\eta}L_{n_{r_\perp}-2}\right] \quad \text{(B5)}$$

We rewrite the last term in (B5) using relation

$$(n+1)L_{n-2}(x)=(2n-1-x)L_{n-1}(x)-nL_n(x), \quad \text{(B6)}$$

and we get

$$e^{-\eta/2}\left[\left(\eta-2-4n+\frac{4n^2}{\eta}\right)L_{n_{r_\perp}}+\left(\frac{4n}{\eta}+4n-\frac{8n^2}{\eta}\right)L_{n_{r_\perp}-1}+\frac{4n}{\eta}\left((2n-1-\eta)L_{n_{r_\perp}-1}-nL_{n_{r_\perp}}\right)\right]=$$
$$=e^{-\eta/2}\left[\left(\eta-2-4n+\frac{4n^2}{\eta}-\frac{4n^2}{\eta}\right)L_{n_{r_\perp}}+\left(\frac{4n}{\eta}+4n-\frac{8n^2}{\eta}+\frac{8n^2}{\eta}-\frac{4n}{\eta}-4n\right)L_{n_{r_\perp}-1}\right]=$$
$$=e^{-\eta/2}(\eta-2-4n)L_{n_{r_\perp}}=e^{-\eta/2}\left[(\eta-1-2n)L_{n_{r_\perp}}-(1+2n)L_{n_{r_\perp}}\right] \quad \text{(B7)}$$

Next, using the relation

$$(n+1)L_{n+1}(x)=(2n+1-x)L_n(x)-nL_{n-1}(x), \quad \text{(B8)}$$

we finally obtain for the derivative terms with η

$$\partial_\eta\left(e^{-\eta/2}L_{n_{r_\perp}}(\eta)\right)=e^{-\eta/2}\left(-(n+1)L_{n_{r_\perp}+1}-nL_{n_{r_\perp}-1}-(1+2n)L_{n_{r_\perp}}\right). \quad \text{(B9)}$$

When evaluating the term with derivative with respect to ξ in equation (B1) we use relations for Hermite polynomials

$$\partial_x H_n(x)=2nH_{n-1}(x) \text{ and } xH_n(x)=\frac{1}{2}H_{n+1}(x)+nH_{n-1}(x). \quad \text{(B10)}$$

Then

$$\partial_z^2 \to \frac{1}{b_z^2}\partial_\xi^2$$

$$\partial_\xi^2\left(e^{-\xi^2/2}H_n(\xi)\right)=\partial_\xi^2\left(e^{-\xi^2/2}\right)H_n+2\partial_\xi\left(e^{-\xi^2/2}\right)\partial_\xi(H_n)+e^{-\xi^2/2}\partial_\xi^2=$$

$$=-e^{-\xi^2/2}H_n+\xi^2e^{-\xi^2/2}H_n-2\xi e^{-\xi^2/2}2nH_{n-1}+e^{-\xi^2/2}4n(n-1)H_{n-2}=$$

$$=e^{-\xi^2/2}\left[\left(-1+\xi^2\right)H_n-4n\xi H_{n-1}+4n(n-1)H_{n-2}\right]=$$

$$=e^{-\xi^2/2}\left[\frac{1}{4}H_{n+2}+\left(n+\frac{1}{2}\right)H_n+n(n-1)H_{n-2}-H_n-4n\left(\frac{1}{2}H_n+(n-1)H_{n-2}\right)+4n(n-1)H_{n-2}\right]=$$

$$=e^{-\xi^2/2}\left[\left(n+\frac{1}{2}-1-2n\right)H_n+\frac{1}{4}H_{n+2}+\left(n(n-1)+4n(n-1)-4n(n-1)\right)H_{n-2}\right]=$$

$$e^{-\xi^2/2}\left[\left(-n-\frac{1}{2}\right)H_n+\frac{1}{4}H_{n+2}+n(n-1)H_{n-2}\right].$$

(B11)

Finally, using (B9) and (B11) we obtain the expression for the matrix elements $H_{n'_z n'_r n_z n_r}$

$$\begin{aligned}H_{n'_z n'_r n_z n_r}=&\left[\frac{1}{b_\perp^2}\left(2n_{r_\perp}+1\right)+\frac{1}{b_z^2}\left(n_z-\frac{1}{2}\right)+m_\phi^2\right]\delta_{n_z,n'_z}\delta_{n_{r_\perp},n'r_{r_\perp}}-\\&-\frac{1}{b_z^2}\frac{1}{2}\left[\sqrt{n'_z(n_z+1)}\delta_{n_z+2,n'_z}+\sqrt{n_z(n'_z+1)}\delta_{n_z-2,n'_z}\right]\delta_{n_{r_\perp},n'_{r_\perp}}+\\&+\frac{1}{b_\perp^2}\left[n'_{r_\perp}\delta_{n_{r_\perp}+1,n'_{r_\perp}}+n_{r_\perp}\delta_{n_{r_\perp}-1,n'_{r_\perp}}\right]\delta_{n_z,n'_z}\end{aligned}\qquad\text{(B12)}$$

References

[1] N. K. Glendenning, Phys. Lett. 114B (1982) 392.

[2] J. Schaffner, I. Mishustin, Phys. Rev. C53 (1996) 1416.

[3] D. Vretenar W. Pöschl, G.A. Lalazissis and P. Ring, Phys. Rev. C57 (1997) 1060.

[4] L. Majling, Proc. of International Conf., "Nucl. Struc. and Related Topic", June 13- 17, 2006, Dubna, Russia.

[5] P. K. Saha, T. Fukuda et al., Phys. Rev. Lett. 94 (2005) 052502.

[6] M. Agnello et al, nucl-ex/0607019.

[7] R. Bertini et al., Phys. Lett. 90B (1980) 375, 136B (1984) 29, 158B (1985) 19.

[8] R.S. Hayano et al. INS-Rep. 705 (sept., 1988), Proceedings of the International Symposium on Hypernuclear and Low-energy Kaon Physics (Padova, 1988), eds. T. Bressani et al., Nuovo Cimento A 102 (1989) 437, Phys. Lett. 213B (1989) 355

[9] T. Yamazaki et al., Phys. Lett. 144B (1984) 177, Phys. Rev. Lett. 54 (1985) 102.

[10] R. Sawafta, Nucl. Phys. A 585 (1993) 103 c.

[11] C. J. Batty, E. Friedman and A. Gal, Phys. Lett. B 335 (1994) 273.

[12] J. Mareš, E. Friedman, A. Gal, B. K. Jennings, Nucl. Phys., A 594 (1995) 311.

[13] B. D. Serot and J. D. Walecka, Advances in Nuclear Physics. 16 (1986) 1.

[14] B. D. Serot, J. D. Walecka, Int. J. Mod. Phys. E6 (1997) 515.

[15] B. K. Jennings, Phys. Lett. B 246 (1990) 325.

[16] J. Mareš, B. K. Jennings, Phys. Rev C, Vol. 49 (1994) 2472.

[17] R. Machleidt, K. Holinde, C. Elster, Phys. Rep. C 149 (1987) 1.

[18]P.-G. Reinhard, Rep. Prog. Phys. 52 (1989) 439.

[19] Y. Sughara, H. Toki, Nucl. Phys A579 (1994) 557.

[20] J. Boguta, A. R. Bodmer, Nucl. Phys. A292 (1977) 413.

[21] N. K. Glendenning, D. Von-Eiff. M. Haft, H. Lenske, and M. K. Weigel, Phys. Rev. C 48 (1993) 889.

[22] W. Greiner, Relativistic Quantum Mechanics–wave equations, 3rd edition, Springer 2000.

[23] Y. K. Gambhir, P. Ring and A. Thimet, Ann. Phys (N.Y.) 198 (1990) 132.

[24] J. Formánek, Úvod do kvantové teorie 1., Academia 2004.

[25] C. J. Horowitz, B.D. Serot, Nucl. Phys., A 368 (1981) 503.

[26] P. G. Reinhard. M. Rufa. J. Maruhn,W. Greiner, and J. Friedrich, Z. Phys. A 323 (1986) 13.

[27] M. M. Sharma, M. A. Nagarajan, and P. Ring, Phys. Lett. B 312 (1993) 377.

[28] C. B. Dover and A. Gal, in Progress in Particle and Nuclear Physics, edited by D. Wilkinson (Pergamon Press, Oxford, 1984), Vol. 12, p. 171.
[29] A. H. Wapstra and G. Audi, Nucl. Phys. A 432 (1985) 1.
[30] H. de Vries, C. W. de Jager and C. de Vries, At. Data Nucl. Data Tables 36 (1987) 495.
[31] H. Tamura, Nucl. Phys. A 721 (2003) 84c.